Supporting Information

Unprecedented J-Aggregated Dyes in Pure Organic Solvents

Hegoi Manzano, Ixone Esnal, Tamara Marqués-Matesanz, Jorge Bañuelos, Iñigo López-Arbeloa, María J. Ortiz, Luis Cerdán, Angel Costela, Inmaculada García-Moreno, Jose Luis Chiara**

Index

1. Supplementary figures.

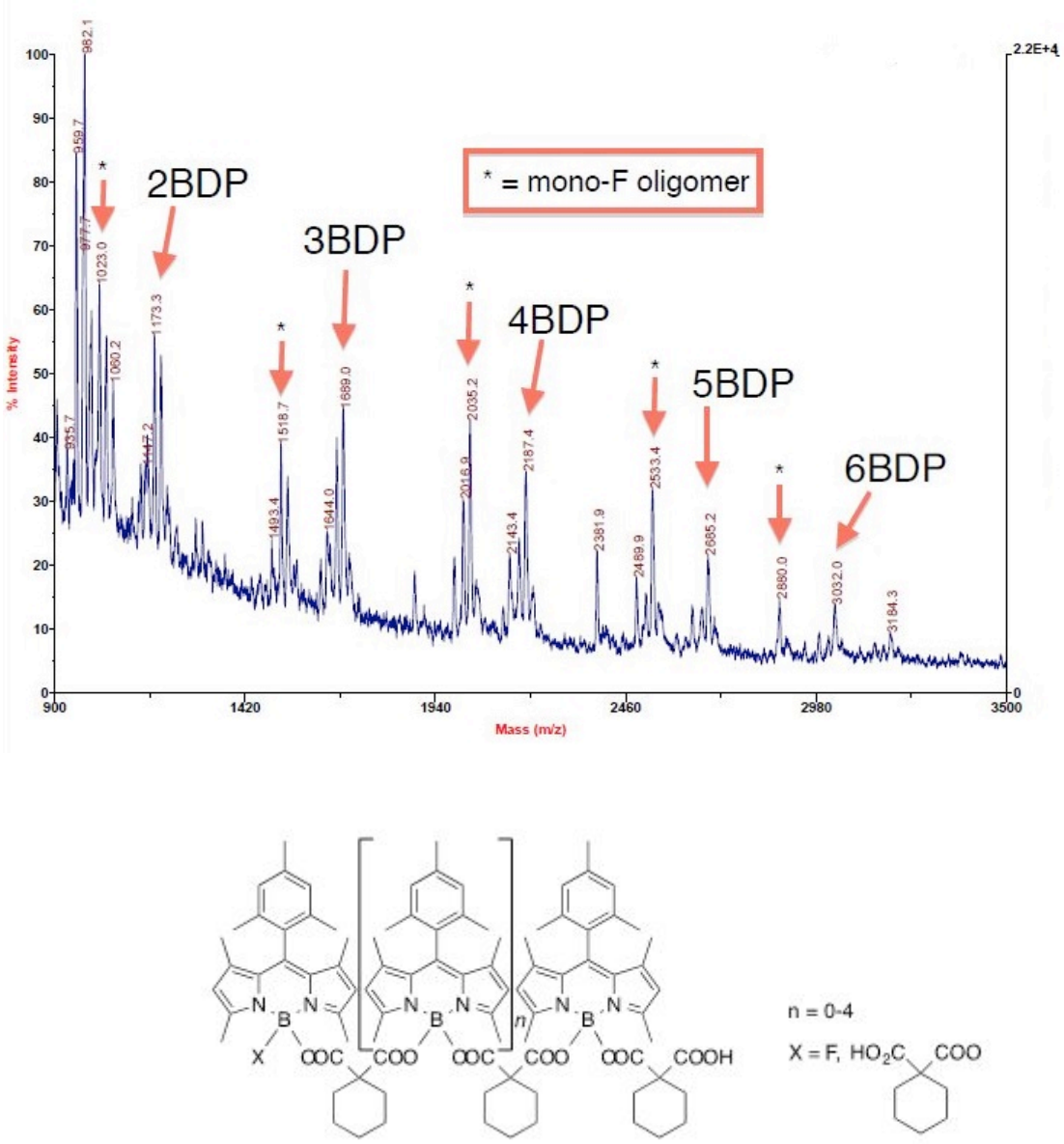

Figure S1. MALDI-TOFF spectrum of the crude reaction mixture of the attempted synthesis of compound **1e**, showing the presence of oligomeric BODIPYs with ciclohexane-1,1-dicarboxylate bridges between units (see structure below; the arrows mark the number of monomeric BODIPYs in the oligomers, which appear in pairs with different X terminal groups).

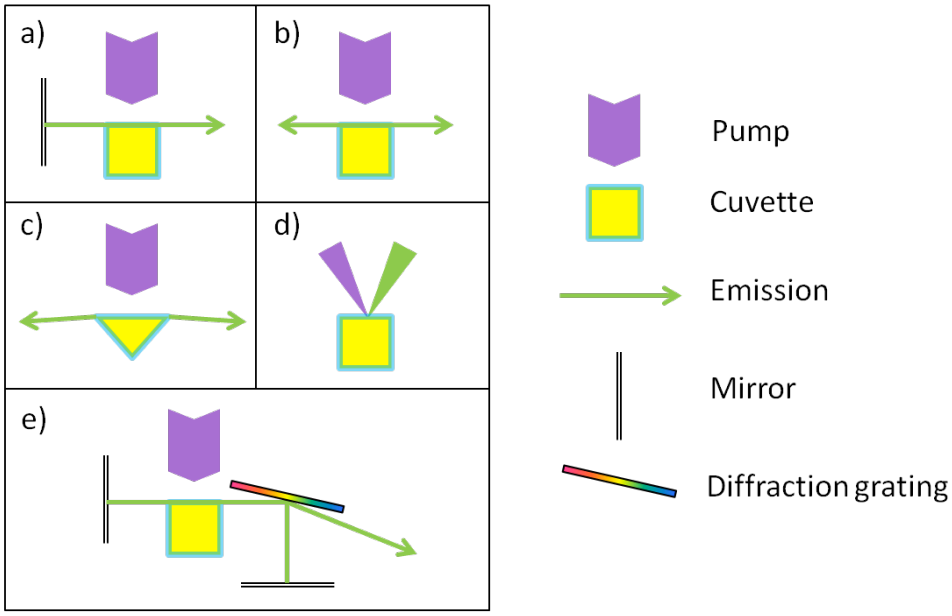

Figure S2. Sketch of cavity/pump configurations used throughout the paper: a) plane-parallel full cavity (2 cm), b) cuvette cavity (1 cm), b) cuvette cavity, c) Triangular quartz cell, d) front-face configuration, and e) tuning cavity.

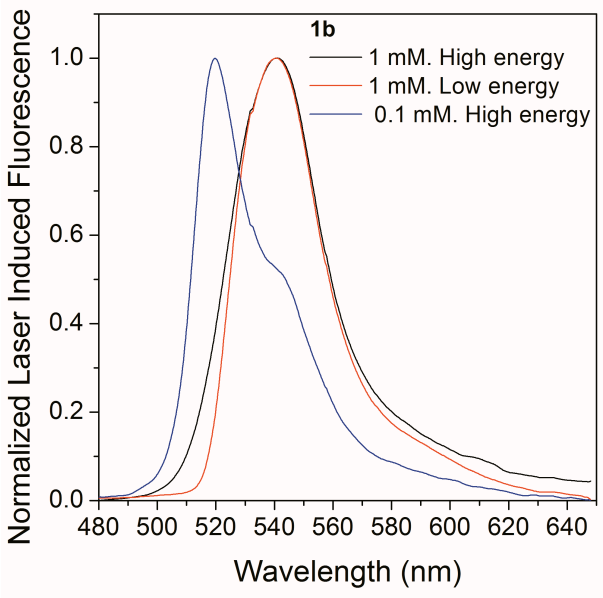

Figure S3. Normalized Laser Induced Fluorescence (LIF) spectra of dye **1b** at different concentrations and pump energies.

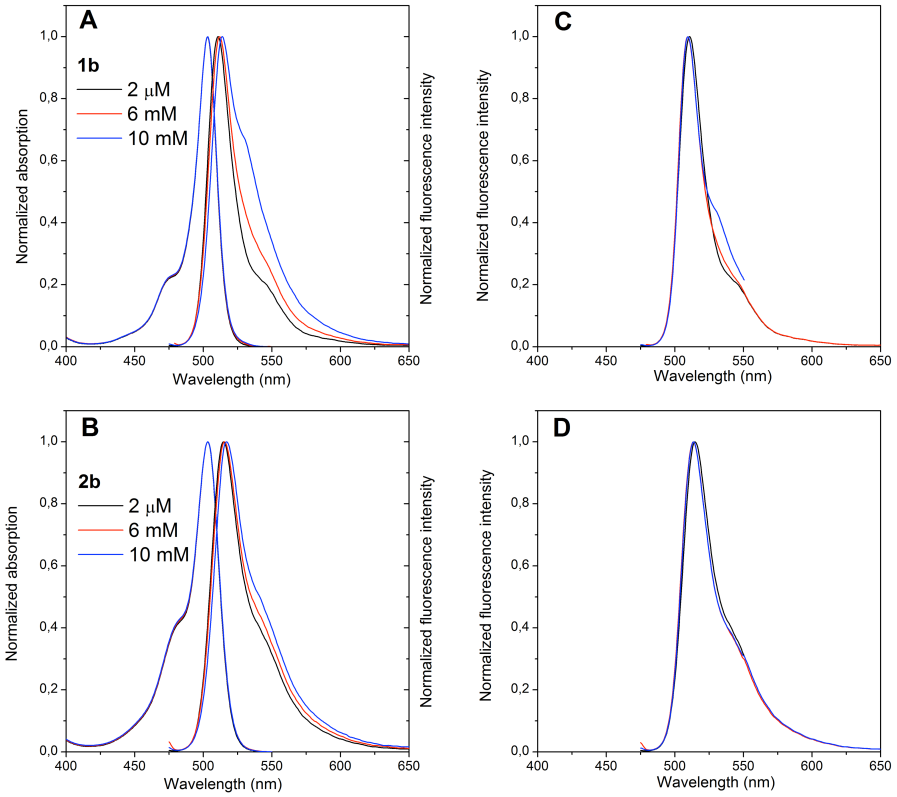

Figure S4. Normalized absorption and fluorescence spectra of dye **1b** (A) and **2b** (B) in diluted (1 cm optical path length) and concentrated (0.001 cm optical path length) solutions in ethyl acetate. Normalized fluorescence spectra after reabsorption correction at high concentration (C and D, respectively).

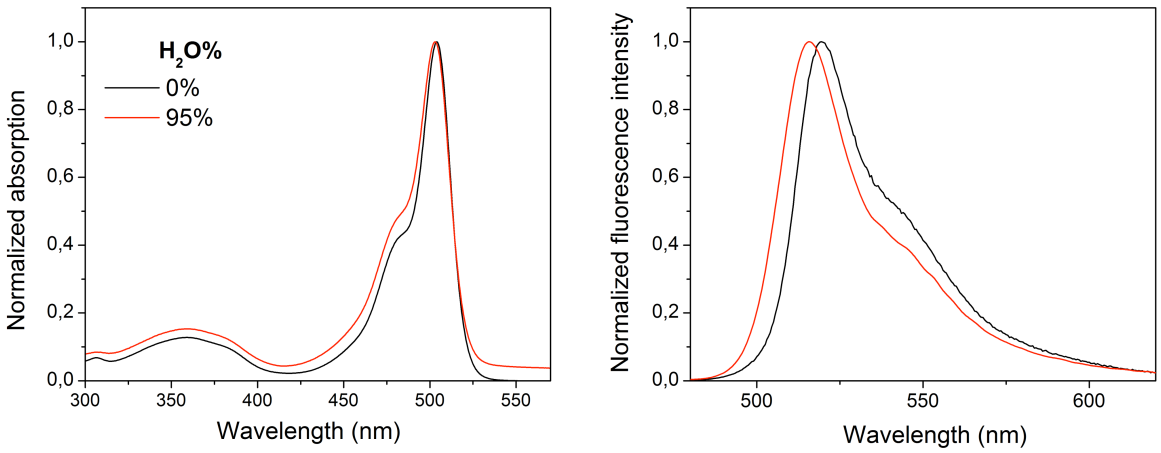

Figure S5. Normalized absorption and fluorescence spectra of **2b** (10 μM) in water-ethanol mixtures to demonstrate that the spectral shape does not change. In water-rich mixtures, the sample is no longer a "true" solution and becomes a colloidal suspension. For this reason, the baseline correction is not good enough in such mixtures.

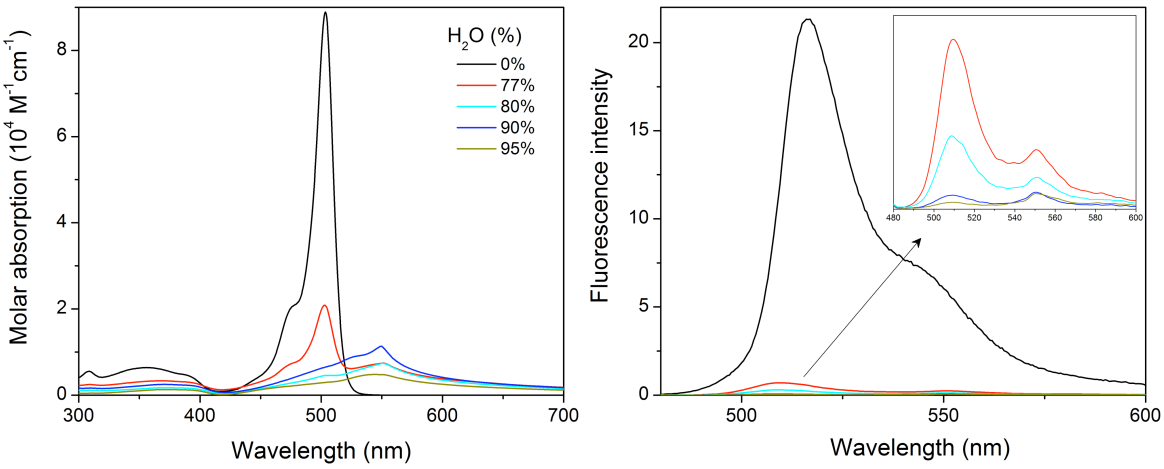

Figure S6. Absorption and fluorescence spectra of dye **1b** in water-ethanol mixtures (10 μM dye concentration).

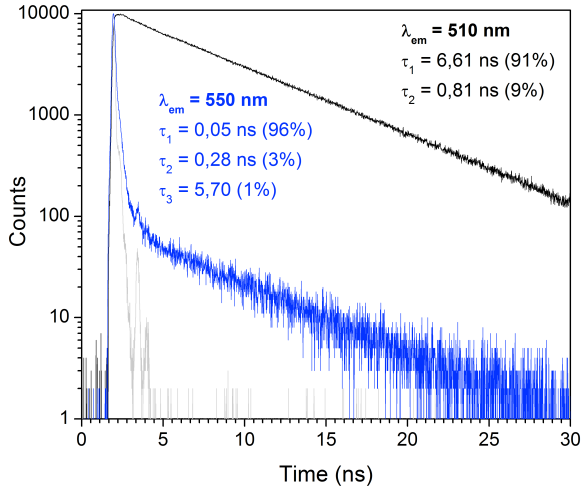

Figure S7. Fluorescence decay curves of **1b** in water-ethanol mixture (90:10 v/v) with a 10 μM dye concentration, exciting at 470 nm and monitoring the emission in both peaks: 510 nm for the monomer and 550 nm for the J-aggregate.

2. General experimental procedures and synthesis of *B*-spiranic *O*-BODIPYs

General. All melting points were measured with a Reicher Jung Thermovar micro-melting apparatus. Proton and carbon-13 nuclear magnetic resonance (^{1}H NMR or ^{13}C NMR) spectra were recorded on a Varian INOVA 400 (400 and 100 MHz, respectively) or a Varian UNITY 500 (500 and 125 MHz, respectively) spectrometers. Chemical shifts are expressed in parts per million (δ scale) downfield from tetramethylsilane and are referenced to residual peaks of the deuterated NMR solvent used or to internal tetramethylsilane. Data are presented as follows: chemical shift, multiplicity (s = singlet, d = doublet, t = triplet, m = multiplet and/or multiple resonances, b = broad), integration, coupling constants in hertz (Hz), and assignment. Proton and carbon-13 assignments are based on DQ-COSY, HSQC, and HMBC correlation experiments. Thin layer chromatography (TLC) was performed with Merck Silica Gel 60 F254 plates. Chromatograms were visualized using UV light (254 nm or 365 nm) and/or treatment with a solution of ammonium molybdate (50 g) and cerium(IV) sulphate (1 g) in 5 % aqueous H_2SO_4 (1 L) followed by charring on a hot plate. Column chromatography was performed on a 971-FP Flash Purification System from Agilent Tecnologies using SF Si35 silica cartridges. Mass spectra of oligomers were recorded on a MALDI Voyager-DE PRO time-of-flight (TOF) spectrometer (Applied Biosystems), using a 2,5-dihydroxybenzoic acid matrix. High-resolution mass spectra (HRMS) were recorded on an Agilent 6520 Q-TOF instrument with an ESI source.

Anhydrous solvents were prepared according to standard methods by distillation over drying agents or via elution through a PureSolv™ column drying system from Innovative Technology, Inc. All other solvents were of HPLC grade and were used as

provided. All reactions were carried out with magnetic stirring and, if air or moisture sensitive, in oven-dried glassware under argon. Microwave irradiation experiments were performed with a single-mode Discover System from CEM Corporation, using standard Pyrex tubes (10 or 35 mL capacity) sealed with a rubber cap.

General method for the synthesis of *O*-BODIPYs by reaction of *F*-BODIPYs with diacids or hydroxyacids. A solution of the starting *F*-BODIPY (0.11 mmol), the diacid or hydroxyacid (0.13 mmol), and trimethylsilyl chloride (2.2 mmol) in dry MeCN (4 mL) was heated under microwave irradiation at 120 ºC for 30 minutes. The solvent and excess volatile reagents were removed at reduced pressure and the crude product was purified by flash column chromatography (hexane/EtOAc) or by crystallization.

Photophysical properties. The absorption and fluorescence spectra, as well as fluorescence decay curves, were measured in diluted solutions (around 2×10^{-6} M) and concentrated solutions (up to 10^{-2} M) of ethyl acetate using quartz cuvettes of different pathway (from 1 cm to 0.01 cm or 0.001 cm, respectively). The water rich mixtures with ethanol were stirred during the measure to avoid flocculation of the suspension. UV-Vis absorption and fluorescence spectra were recorded on a Varian model CARY 4E spectrophotometer and on an Edinburgh Instruments spectrofluorimeter (model FLSP 920), respectively. The fluorescence spectra of diluted samples were measured in right-angle, whereas concentrated ones in front-face to minimize inner filter effects. Fluorescence quantum yields (ϕ) were obtained using PM546 (ϕ^r = 0.85 in ethanol)[1] as reference, with the exception of **3a**, in which PM567 (ϕ^r = 0.84 in ethanol)[1] were employed. These fluorescence efficiencies were calculated from corrected spectra (detector sensibility to the wavelength) and corrected by the refractive index of the solvent. Radiative decay curves

were registered with the time correlated single-photon counting technique (Edinburgh Instruments, model FL900, with picosecond time-resolution). Fluorescence emission was monitored at the maximum emission wavelength after excitation at 470 nm by means of a diode laser (PicoQuant LDH470) with a repetition rate of 10 MHz. The fluorescence lifetime (τ) was obtained from the slope of an exponential fit after the deconvolution of the instrumental response signal from the recorded decay curves by means of an iterative method. The goodness of the exponential fit was controlled by statistical parameters (chi-square, Durbin-Watson and the analysis of the residuals).

Fluorescence images in the solid state were recorded with an optical inverted microscope with epi configuration (Olympus BX51) equipped with a color CCD camera (DP72, Olympus). Crystals were excited under blue light by Chroma band pass filters (D470/40) and the emission was collected with Chroma cut-off filters (E515LPv2). The corresponding spectra were registered coupling the microscope to the aforementioned spectrofluorimeter by an optical fiber. Absolute fluorescence quantum yields were measured by means of an integrated sphere coupled to the spectrofluorimeter.

Atomistic simulation. The generic DREIDING force field[2] was used to model the short-range and van der Waals interactions, while the long-range interactions were computed by a coulombic potential. The atomic charges were obtained from Density Functional Theory (DFT) simulations as implemented in the Gaussian09[3] using the B3LYP exchange correlation functional and a 6-311G+ basis set. The internal structure of the dyes were relaxed to a local minimum of energy, and the charges were computed under the ChelpG scheme.[4] Molecular Dynamics simulations were carried out using the LAMMPS package (05Sep14 version)[5] in the NPT ensemble at room temperature and pressure conditions.

The calculations were done using the Nose-Hoover style equations of motions derived by Shinoba et al.,[6] with a timestep of 1fs and thermostating and barostating constants of 100 and 1000 fs respectively. The long range interactions were computed using the particle-particle particle-mesh method.[7] The solvent boxes were prepared placing randomly the desired number of molecules with Packmol,[8] and probability analyses of the trayectories were done using Travis.[9]

Lasing properties. Liquid solutions of dyes were contained in 1 cm optical-path rectangular quartz cells carefully sealed to avoid solvent evaporation during experiments. The liquid solutions were transversely pumped at 355 nm, with 5 mJ, 8 ns FWHM pulses from the third-harmonic of *Q*-switched Nd:YAG laser (Spectron SL282G), at a repetition rate of up to 10 Hz. The exciting pulses were line-focused onto the cell, providing pump fluences on the active medium in the range 110 - 180 mJ/cm^2. The oscillation cavity (2 cm length) consisted of a 90% reflectivity aluminum mirror, with the lateral face of the cell as output coupler. Narrow-linewidth laser emission and tuning ranges of dye solutions were obtained by placing the samples in a home-made Shoshan-type oscillator (Figure S2e) consisting of full-reflecting aluminium back and tuning mirrors, and a 2400 lines mm^{-1} holographic grating in grazing incidence, with outcoupling via the grating zero order.[10] Wavelength tuning was accomplished by rotation of the tuning mirror. Tuning mirror and grating (both from Optometrics) were 5 cm wide and the angle of incidence on the grating was 88.5°. Laser linewidth was measured with a Fabry-Perot etalon (IC Optical Systems) with a free spectral range of 15.9 GHz.

X-ray diffraction studies. Intensity data were collected on an Agilent Technologies Super-Nova diffractometer, wich was equipped with monochromated Cu kα radiation (λ= 1.54184

Å) and Atlas CCD detector. Measurement was carried out at 99.99(10) K with the help of an Oxford Cryostream 700 PLUS temperature device. Data frames were processed (united cell determination, analytical absorption correction with face indexing, intensity data integration and correction for Lorentz and polarization effects) using the Crysalis software package.[11] The structure was solved using Olex2[12] and refined by full-matrix least-squares with SHELXL-97.[13] Final geometrical calculations were carried out with Mercury[14] and PLATON[15] as integrated in WinGX.[16] Crystallographic data (excluding structure factors) for the structure(s) reported in this paper have been deposited with the Cambridge Crystallographic Data Centre as supplementary publication no. CCDC-1411347-1411349 and CCDC-1411353-1411358. Copies of the data can be obtained free of charge from www.ccdc.cam.ac.uk/conts/retrieving.html.

Synthesis of *O*-BODIPY 1a. Reaction of *F*-BODIPY **1** (30 mg, 0.082 mmol) with malonic acid (9 mg, 0.086 mmol) following the general method for the synthesis of *O*-BODIPYs gave **1a** (33 mg, 94%) as a dark-red solid, after flash chromatography purification (hexane/EtOAc 76:24 → 41:59).

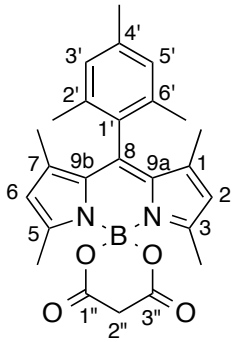

1a

Mp 115-118 ºC. ^{1}H NMR ($CDCl_3$, 500 MHz): δ = 1.39 (s, 6H, CH_3-C1, CH_3-C7), 2.09 (s, 6H, CH_3-C2', CH_3-C6'), 2.31 (s, 6H, CH_3-C3, CH_3-C5), 2.34 (s, 3H, CH_3-C4'), 3.65 (s, 2H, C2"H_2), 5.99 (s, 2H, C2H, C6H), 6.96 (s, 2H, C3'H, C5'H). ^{13}C NMR ($CDCl_3$, 125 MHz): δ

= 13.8 (*C*H$_3$-C1, *C*H$_3$-C7), 15.1 (*C*H$_3$-C3, *C*H$_3$-C5), 19.7 (*C*H$_3$-C2', *C*H$_3$-C6'), 21.4 (*C*H$_3$-C4'), 37.9 (C2''), 122.5 (C2, C6), 129.4 (C3', C5'), 130.6 (C1'), 131.5 (C1,C7), 134.8 (C2', C6'), 139.2 (C4'), 143.0 (C8), 144.0 (C9a, C9b), 154.4 (C3, C5), 166.8 (2×C=O). HRMS (API-ES$^+$): calcd for $C_{25}H_{28}BN_2O_4$ (M+H)$^+$: 431.2142, found: 431.2147.

Synthesis of *O*-BODIPY 1b. Reaction of *F*-BODIPY **1** (37 mg, 0.101 mmol) with cyclopropane-1,1-dicarboxylic acid (15 mg, 0.115 mmol) following the general method for the synthesis of *O*-BODIPYs gave **1b** (39 mg, 85%) as a dark-red solid, after flash chromatography purification (hexane/EtOAc 100:0 → 80:20).

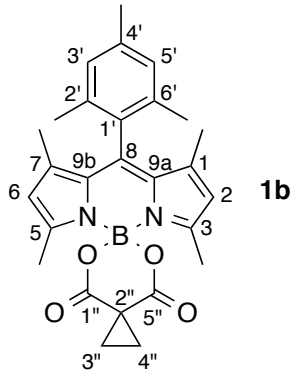

1b

Mp 242-245 ºC. ^{1}H NMR ($CDCl_3$, 500 MHz): δ = 1.39 (s, 6H, CH_3-C1, CH_3-C7), 1.93 (s, 4H, C3"H_2, C4"H_2), 2.09 (s, 6H, CH_3-C2', CH_3-C6'), 2.34 (s, 3H, CH_3-C4'), 2.37 (s, 6H, CH_3-C3, CH_3-C5), 5.99 (s, 2H, C2H, C6H), 6.96 (s, 2H, C3'H, C5'H). ^{13}C NMR ($CDCl_3$, 125 MHz): δ = 13.7 (*C*H$_3$-C1, *C*H$_3$-C7), 15.1 (*C*H$_3$-C3, *C*H$_3$-C5), 19.7 (*C*H$_3$-C2', *C*H$_3$-C6'), 21.4 (*C*H$_3$-C4'), 23.8 (C3", C4"), 25.6 (C2"), 122.3 (C2, C6), 129.3 (C3', C5'), 130.8 (C1'), 131.4 (C1, C7), 134.9 (C2', C6'), 139.1 (C4'), 142.7 (C8), 143.7 (C9a, C9b), 154.7 (C3, C5), 171.0 (2×C=O). HRMS (API-ES$^+$): calcd. for $C_{27}H_{30}BN_2O_4$ (M+H)$^+$: 457.2298, found: 457.2299.

Synthesis of *O*-BODIPY 1c. Reaction of *F*-BODIPY **1** (40 mg, 0.109 mmol) with cyclobutane-1,1-dicarboxylic acid (21 mg, 0.146 mmol) following the general method for the synthesis of *O*-BODIPYs gave **1c** (50 mg, 98%) as a dark-red solid, after flash chromatography purification (hexane/EtOAc 100:0 → 50:50).

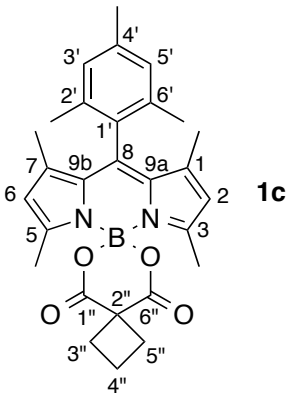

Mp. 253-255 ºC. ^{1}H NMR ($CDCl_3$, 400 MHz): δ = 1.37 (s, 6H, CH_3-C1, CH_3-C7), 2.07 (s, 6H, CH_3-C2', CH_3-C6'), 2.19 (s, 6H, CH_3-C3, CH_3-C5), 2.33 (s, 3H, CH_3-C4'), 2.42 (m, 2H, C4"H_2), 2.78 (m, 4H, C3"H_2, C5"H_2), 5.95 (s, 2H, C2H, C6H), 6.95 (s, 2H, C3'H, C5'H). ^{13}C NMR ($CDCl_3$, 100 MHz): δ = 13.7 (*C*H_3-C1, *C*H_3-C7), 15.2 (*C*H_3-C3, *C*H_3-C5), 16.4 (C4"), 19.7 (*C*H_3-C2', *C*H_3-C6'), 21.4 (*C*H_3-C4'), 31.4 (C3", C5"), 47.5 (C2"), 122.3 (C2, C6), 129.3 (C3', C5'), 130.7 (C1'), 131.4 (C1, C7), 134.9 (C2', C6'), 139.1 (C4'), 142.8 (C8), 143.6 (C9a, C9b), 154.3 (C3, C5), 174.6 (2×C=O). HRMS (API-ES$^+$): calcd. for $C_{28}H_{32}BN_2O_4$ $(M+H)^+$: 471.2455, found: 471.2445.

Synthesis of *O*-BODIPY 1d. Reaction of *F*-BODIPY **1** (40 mg, 0.109 mmol) with cyclopentane-1,1-dicarboxylic acid (22 mg, 0.139 mmol) following the general method for the synthesis of *O*-BODIPYs (microwave irradiation time = 45 min) gave **1d** (39 mg, 74%) as a dark-red solid, after recrystallization of the crude evaporated reaction mixture from MeCN at 5 ºC.

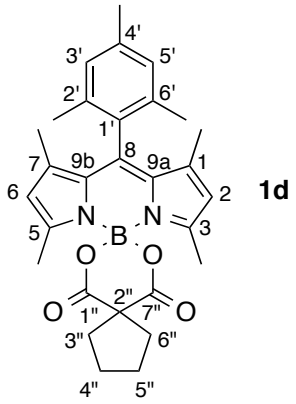

1d

Mp. 267-270 ºC. ^{1}H NMR ($CDCl_3$, 500 MHz): δ = 1.37 (s, 6H,CH_3-C1, CH_3-C7), 2.04 (m, 4H, CH_3-C4", CH_3-C5"), 2.08 (s, 6H, CH_3-C2', CH_3-C6'), 2.33 (s, 3H, CH_3-C4'), 2.35 (s, 3H, CH_3-C3, CH_3-C5), 2.39 (m, 4H, C3"H_2, C6"H_2), 5.96 (s, 2H, C2H, C6H), 6.96 (s, 2H, C3'H, C5'H). ^{13}C NMR ($CDCl_3$, 125 MHz): δ = 13.8 (*C*H_3-C1, *C*H_3-C7), 16.1 (*C*H_3-C3, *C*H_3-C5), 19.7 (*C*H_3-C2', *C*H_3-C6'), 21.4 (*C*H_3-C4'), 28.6 (C4", C5"), 42.1 (C3", C6"), 54.6 (C2"), 122.4 (C2, C6), 129.3 (C3', C5'), 130.8 (C1'), 131.6 (C1, C7), 134.9 (C2', C6'), 139.1 (C4'), 142.7 (C8), 143.7 (C9a, C9b), 154.6 (C3, C5), 176.8 (2×C=O). HRMS (API-ES$^+$): calcd. for $C_{29}H_{34}BN_2O_4$ $(M+H)^+$: 485.2612, found: 485.2588.

Synthesis of *O*-BODIPY 1g. Reaction of *F*-BODIPY **1** (30 mg, 0.082 mmol) with oxalic acid (8 mg, 0.089 mmol) following the general method for the synthesis of *O*-BODIPYs gave **1g** (33 mg, 97%) as a dark-red solid, after flash chromatography purification (hexane/EtOAc 94:6 → 70:30).

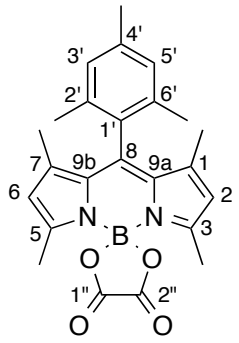

1g

Mp. 205-207 ºC. ^{1}H NMR ($CDCl_3$, 500 MHz): δ = 1.42 (s, 6H, CH_3-C1, CH_3-C7), 2.10 (s, 6H, CH_3-C2', CH_3-C6'), 2.30 (s, 6H, CH_3-C3, CH_3-C5), 2.35 (s, 3H, CH_3-C4'), 6.03 (s, 2H, C2H, C6H), 6.99 (s, 2H, C3'H, C5'H). ^{13}C NMR ($CDCl_3$, 125 MHz): δ = 13.8 (CH$_3$-C1, CH$_3$-C7), 15.7 (CH$_3$-C3, CH$_3$-C5), 19.7 (CH$_3$-C2', CH$_3$-C6'), 21.4 (CH$_3$-C4'), 123.2 (C2, C6), 129.5 (C3',C5'), 130.3 (C1'), 131.9 (C1, C7), 134.7 (C2', C6'), 139.4 (C4'), 143.2 (C8), 145.1 (C9a, C9b), 155.8 (C3, C5), 159.9 (2×C=O). HRMS (API-ES$^+$): calcd. for $C_{24}H_{26}BN_2O_4$ $(M+H)^+$: 417.1986, found: 417.1975.

Synthesis of *O*-BODIPY 1h. Reaction of *F*-BODIPY **1** (35 mg, 0.096 mmol) with salicilic acid (15 mg, 0.109 mmol) following the general method for the synthesis of *O*-BODIPYs gave **1h** (39 mg, 87%) as a dark-red solid, after flash chromatography purification (hexane/EtOAc 100:0 → 80:20).

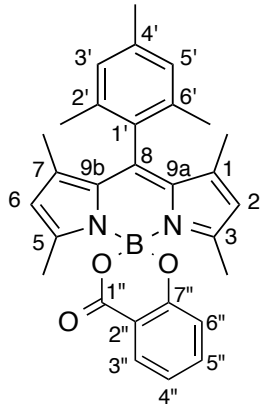

1h

Mp. 278-280 ºC. ^{1}H NMR ($CDCl_3$, 500 MHz): δ = 1.39 (s, 6H, CH_3-C1, CH_3-C7), 2.12 (s, 3H, CH_3-C6'), 2.13 (s, 6H, CH_3-C3, CH_3-C5), 2.15 (s, 3H, CH_3-C2'), 2.34 (s, 3H, CH_3-C4'), 5.94 (s, 2H, C2H, C6H), 6.93 (dd, *J* = 0.7, 8.3 Hz, 1H, C6"H), 6.96 (s, 2H, C3'H, C5'H), 6.98 (dd, *J* = 0.9, 7.8 Hz, 1H, C4"H), 7.49 (ddd, *J* = 1.8, 7.3, 8.3 Hz, 1H, C5"H), 8.08 (dd, *J* = 1.7, 7.8 Hz, 1H, C3"H). ^{13}C NMR ($CDCl_3$, 125 MHz): δ = 13.7 (CH$_3$-C1, CH$_3$-C7), 15.6 (CH$_3$-C3, CH$_3$-C5), 19.8 (CH$_3$-C2', CH$_3$-C6'), 21.4 (CH$_3$-C4'), 115.6 (C2"), 117.7 (C6"), 119.8 (C4"), 122.0 (C2, C6), 129.1 (C5'), 129.3 (C3'), 130.2 (C3"), 131.1 (C1, C7), 131.3 (C1'), 134.9 (C6'), 135.2 (C2'), 135.9 (C5"), 138.9 (C4'), 142.2 (C8), 143.1 (C9a, C9b), 155.8 (C3, C5), 159.8 (C7"), 164.3 (C=O). HRMS (API-ES$^+$): calcd. for $C_{29}H_{30}BN_2O_3$, $(M+H)^+$: 465.2349, found: 465.2358.

Synthesis of *O*-BODIPY 2b. Reaction of *F*-BODIPY **2** (40 mg, 0.129 mmol) with cyclopropane-1,1-dicarboxylic acid (22 mg, 0.169 mmol) following the general method for the synthesis of *O*-BODIPYs gave **2b** (46 mg, 89%) as a dark-red solid, after flash chromatography purification (hexane/EtOAc 100:0 → 60:40).

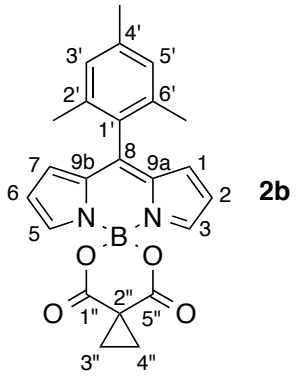

2b

Mp. 262-264 ºC. ^{1}H NMR ($CDCl_3$, 500 MHz): δ = 1.99 (s, 4H, C3"H_2, C4"H_2), 2.11 (s, 6H, CH_3-C2', CH_3-C6'), 2.37 (s, 3H, CH_3-C4'), 6.51 (dd, *J* = 2.0, 4.2 Hz, 2H, C2H, C6H), 6.75 (s, 2H, C1H, C7H), 6.97 (s, 2H, C3'H, C5'H), 7.76 (s, 2H, C3H, C5H). ^{13}C NMR ($CDCl_3$,

125 MHz): δ = 20.2 (*C*H$_3$-C2', *C*H$_3$-C6'), 21.3 (*C*H$_3$-C4'), 23.7 (C3", C4"), 24.7 (C2"), 119.4 (C2, C6), 128.4 (C3', C5'), 129.2 (C1'), 131.4 (C1, C7), 135.5 (C9a, C9b), 136.4 (C2', C6'), 139.4 (C4'), 144.3 (C3, C5), 148.8 (C8), 170.2 (2×C=O). HRMS (API-ES$^+$): calcd. for $C_{23}H_{22}BN_2O_4$ (M+H)$^+$: 401.1673, found 401.1665.

Synthesis of *O*-BODIPY 2e. Reaction of *F*-BODIPY **2** (40 mg, 0.129 mmol) with cyclohexane-1,1-dicarboxylic acid (27 mg, 0.157 mmol) following the general method for the synthesis of *O*-BODIPYs gave **2e** (34 mg, 60%) as a dark-red solid, after flash chromatography purification (hexane/EtOAc 100:0 → 80:20).

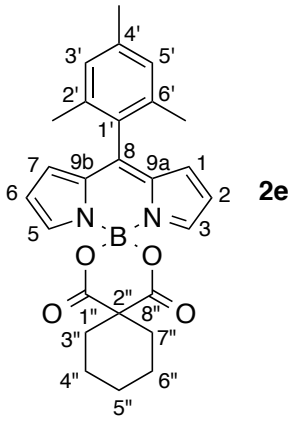

2e

Mp. 244-246 ºC. ^{1}H NMR ($CDCl_3$, 500 MHz): δ = 1.61 (m, 2H, C5"H$_2$), 1.88 (m, 4H, C4"H$_2$, C6"H$_2$), 2.10 (s, 6H, CH$_3$-C2', CH$_3$-C6'), 2.20 (m, 4H, C3"H$_2$, C7"H$_2$), 2.36 (s, 3H, CH$_3$-C4'), 6.47 (dd, *J* = 2.4, 3.9 Hz, 2H, C2H, C6H), 6.72 (d, *J* = 4.1 Hz, 2H, C1H, C7H), 6.96 (s, 2H, C3'H, C5'H), 7.65 (s, 2H, C3H, C5H). ^{13}C NMR ($CDCl_3$, 125 MHz): δ = 20.2 (*C*H$_3$-C2', *C*H$_3$-C6'), 21.3 (*C*H$_3$-C4'), 21.7 (C4", C6"), 24.9 (C5"), 33.4 (C3", C7"), 50.8 (C2"), 119.2 (C2, C6), 128.4 (C3', C5'), 129.3 (C1'), 131.4 (C1, C7), 135.6 (C9a, C9b), 136.5 (C2', C6'), 139.3 (C4'), 144.1 (C3, C5), 148.6 (C8), 172.8 (2×C=O). HRMS (API-ES$^+$) calcd. for $C_{26}H_{28}BN_2O_4$ (M+H)$^+$: 443.2142, found: 443.2141.

Synthesis of *O*-BODIPYs 2i and 2j. Reaction of *F*-BODIPY **2** (40 mg, 0.129 mmol) with chloroacetic acid (32 mg, 0.338 mmol) following the general method for the synthesis of *O*-BODIPYs gave **2i** (6.1 mg, 12%) and **2j** (39 mg, 66%) as dark-red and orange solids, respectively, after flash chromatography purification (hexane/EtOAc 100:0 → 80:20).

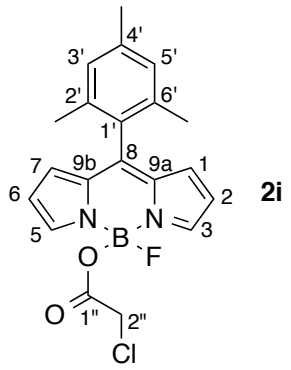

2i

Mp. 36-39 ºC. ^{1}H NMR ($CDCl_3$, 500 MHz): δ = 2.09 (s, 3H, CH_3-C2'), 2.18 (s, 3H, CH_3-C6'), 2.36 (s, 3H, CH_3-C4'), 4.03 (s, 2H, C2"H_2), 6.47 (dd, *J* = 1.9, 4.2 Hz, 2H, C6H, C2H), 6.71 (d, *J* = 4.2 Hz, 2H, C1H, C7H), 6.95 (s, 1H, C3'H), 6,97(s, 1H, C5'H), 7.91 (s, 2H, C3H, C5H). ^{13}C NMR ($CDCl_3$, 125 MHz): δ = 20,12 (*C*H_3-C2'), 20.14 (*C*H3-C6'), 21,3 (*C*H_3-C4'), 42,9 (C2"), 118,8 (C2, C6), 128,2 (C3'), 128,4 (C5'), 129,7 (C1'), 130,5 (C1, C7), 136,0 (C9a, C9b), 136,3 (C2'), 137,1 (C6'), 139.0 (C4'), 144,6 (C3, C5), 148,4 (C8), 167,2 (C=O). HRMS (API-ES$^+$): calcd. for $C_{20}H_{20}BFClN_2O_2$ $(M+H)^+$: 385,1290, found: 459.1036.

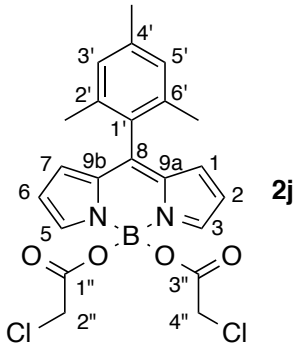

2j

Mp. 175-178 ºC. ^{1}H NMR ($CDCl_3$, 500 MHz): δ = 2.17 (s, 6H, CH_3-C2', CH_3-C6'), 2.36 (s, 3H, CH_3-C4'), 4.07 (s, 4H, C2"H_2, C4"H_2), 6.46 (dd, *J* = 2.0, 4.2 Hz, 2H, C6H, C2H), 6.72 (d, *J* = 4.2 Hz, 2H, C1H, C7H), 6.96 (s, 2H, C3'H, C5'H), 7.90 (s, 2H, C3H, C5H). ^{13}C NMR ($CDCl_3$, 125 MHz): δ = 20,1 (*C*H_3-C2', *C*H_3-C6'), 21,3 (*C*H_3-C4'), 42,8 (C2", C4"), 118,9 (C2, C6), 128,2 (C3', C5'), 129,7 (C1'), 130,6 (C1, C7), 136,5 (C9a, C9b), 136,9 (C2', C6'), 139.0 (C4'), 144,4 (C3, C5), 148,8 (C8), 167,2 (2×C=O). HRMS (API-ES$^+$): calcd. for $C_{22}H_{22}BCl_2N_2O_4$ $(M+H)^+$: 459.1049, found: 459.1036.

Synthesis of *O*-BODIPY 3a. Reaction of *F*-BODIPY **3** (40 mg, 0.087 mmol) with malonic acid (11 mg, 0.106 mmol) following the general method for the synthesis of *O*-BODIPYs gave **3a** (31 mg, 68%) as a dark-red solid, after flash chromatography purification (hexane/EtOAc 100:0 → 80:20).

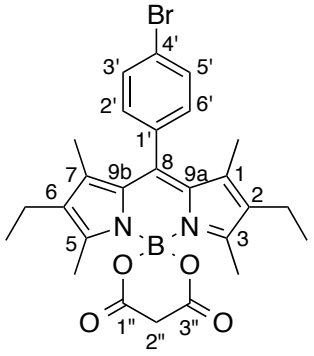

3a

Mp. 265-268 ºC. ¹H NMR ($CDCl_3$, 500 MHz): δ = 0.95 (t, *J* = 7.6 Hz, 6H, C*H*$_3$-CH_2-C2, C*H*$_3$-CH_2-C6), 1.33 (s, 6H, CH_3-C1, CH_3-C7), 2.26 (s, 6H, CH_3-C3, CH_3-C5), 2.29 (c, *J* = 7,6 Hz, 4H, CH_3-C*H*$_2$-C2, CH_3-C*H*$_2$-C6), 3.65 (s, 2H, C2"H_2), 7.17 (d, *J* = 8.4 Hz, 2H, C2'H, C6'H), 7.67 (d, *J* = 8.4 Hz, 2H, C3'H, C5'H). ¹³C NMR ($CDCl_3$, 125 MHz): δ = 12.4 (*C*H_3-C1, *C*H_3-C7), 12.7 (*C*H_3-C3, *C*H_3-C5), 14.7 (*C*H_3-CH_2-C2, *C*H_3-CH_2-C6), 17.2 (CH_3-*C*H_2-C2, CH_3-*C*H_2-C6), 38.0 (C2"), 123.6 (C4'), 130.1 (C2', C6'), 131.5 (C9a, C9b), 132.8 (C3', C5'), 134.3 (C1'), 134.4 (C2, C6), 139.6 (C8), 140.2 (C1, C7), 153.3 (C3, C5),

166.7 (2×C=O). HRMS (API-ES$^+$): calcd. for $C_{26}H_{29}BBrN_2O_4$ $(M+H)^+$: 523.1404, found: 523.1353.

Synthesis of *O*-BODIPY 4a. Reaction of *F*-BODIPY **4** (40 mg, 0.138 mmol) with malonic acid (16 mg, 0.154 mmol) following the general method for the synthesis of *O*-BODIPYs gave **4a** (36 mg, 74%) as a dark-red solid, after recrystallization of the crude evaporated reaction mixture from MeCN/EtOAc.

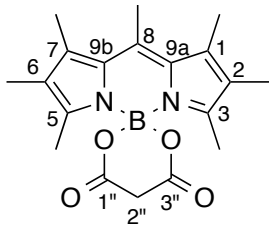

4a

Mp. 259-262 ºC. ^{1}H NMR ($CDCl_3$, 500 MHz): δ = 2.28 (s, 6H, CH_3-C3, CH_3-C5), 2.43 (s, 6H, CH_3-C1, CH_3-C7), 2.62 (s, 3H, CH_3-C8), 3.59 (s, 2H, CH_2-C2''), 6.09 (s, 2H, CH-C2, CH-C6). ^{13}C NMR ($CDCl_3$, 125 MHz): δ = 15.0 (*C*H_3-C3, *C*H_3-C5), 16.8 (*C*H_3-C8), 17.7 (*C*H_3-C1, *C*H_3-C7), 37.9 (C2''), 123.0 (C2, C6), 133.0 (C1, C7), 142.5 (C8), 142.8 (C9a, C9b), 152.8 (C3, C5), 166.6 (2×C=O). HRMS (API-ES$^+$): calcd. for $C_{17}H_{20}BN_2O_4$ $(M+H)^+$: 327.1516, found: 327.1519.

3. X-Ray diffraction structures and Table S1

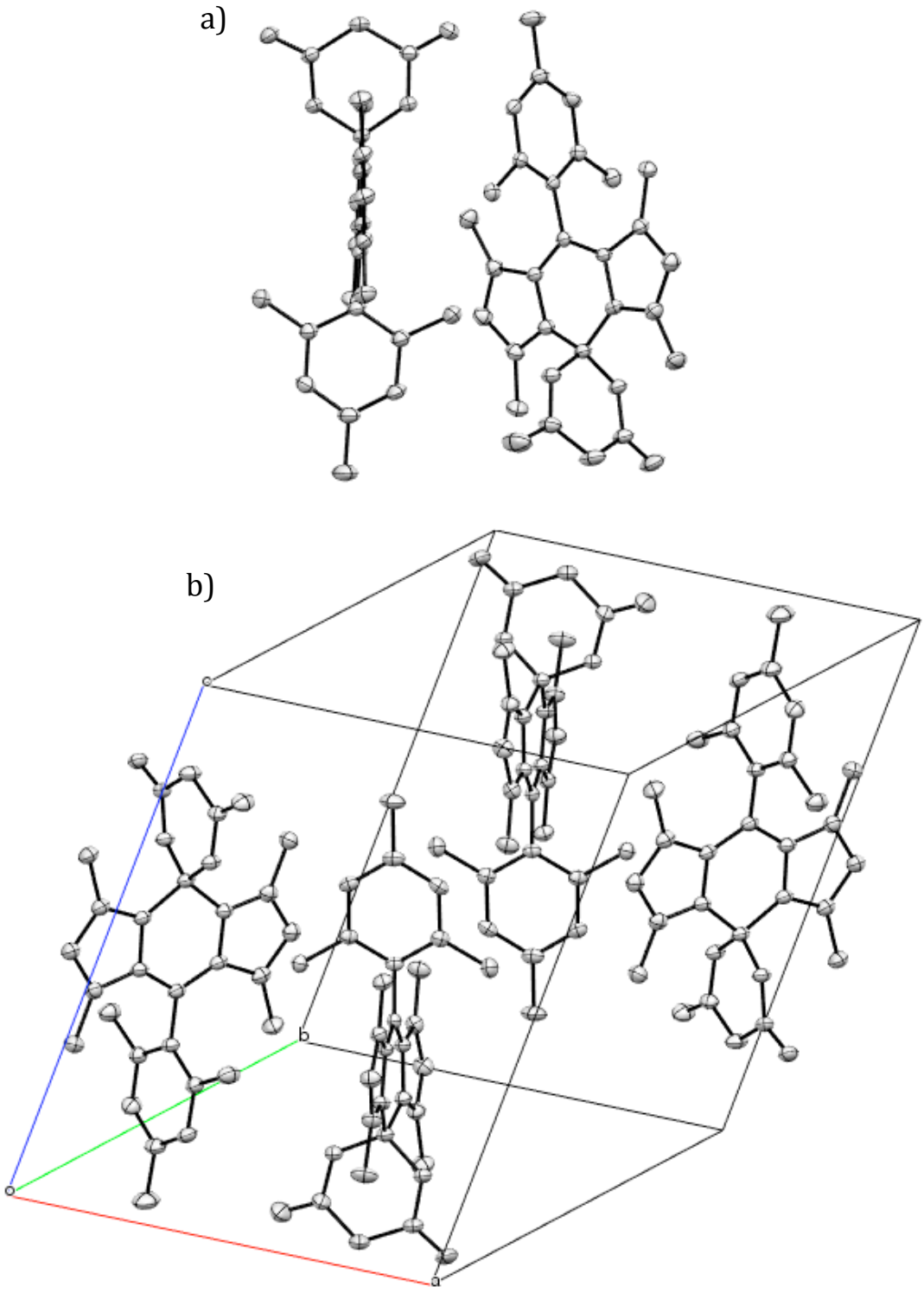

Compound **1a**. (a) Two independent molecules in the crystal cell. (b) Crystal packing diagram.

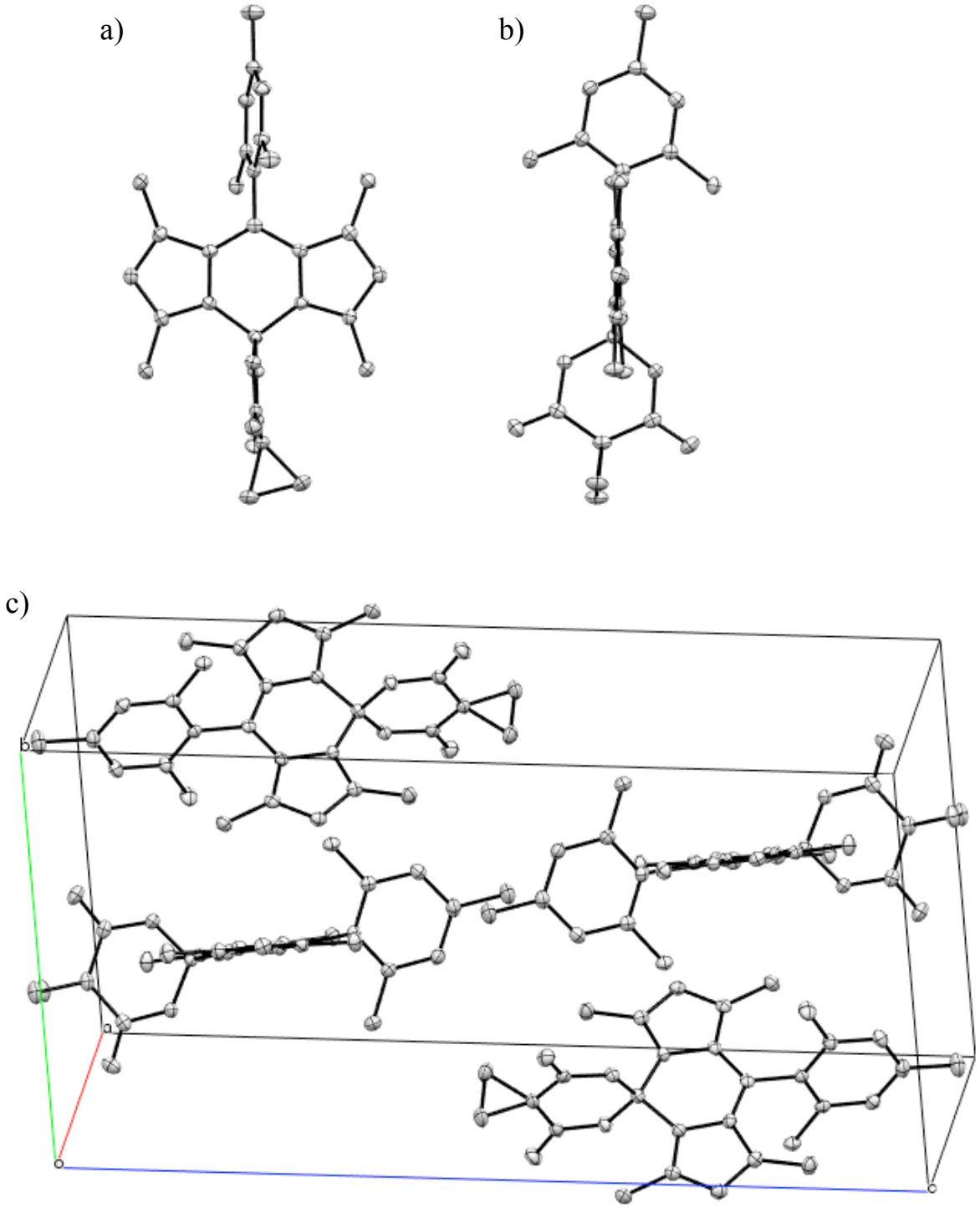

Compound **1b**. (a) Top view. (b) Side view. (c) Crystal packing diagram.

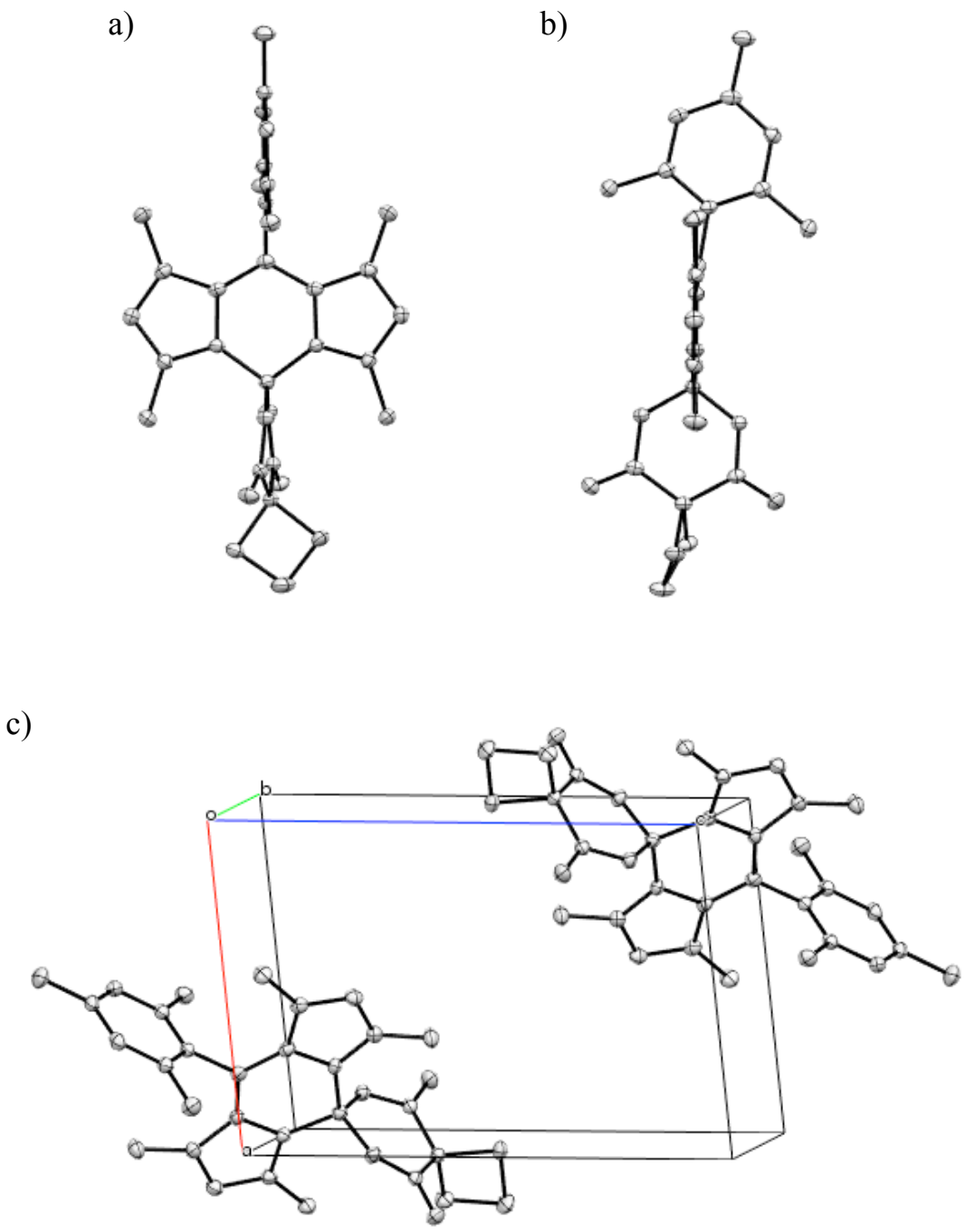

Compound **1c**. (a) Top view. (b) Side view. (c) Crystal packing diagram.

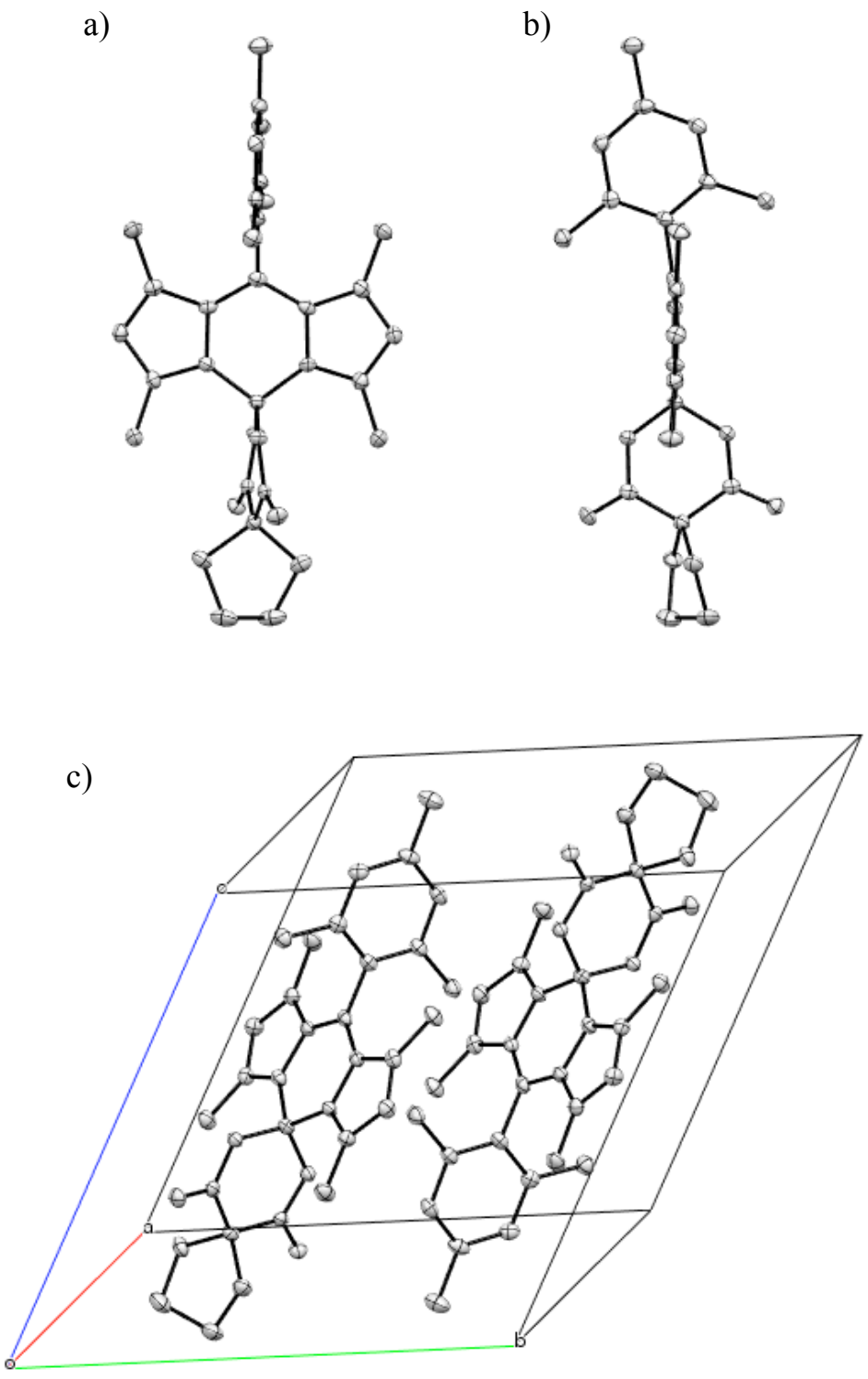

Compound **1d**. (a) Top view. (b) Side view. (c) Crystal packing diagram.

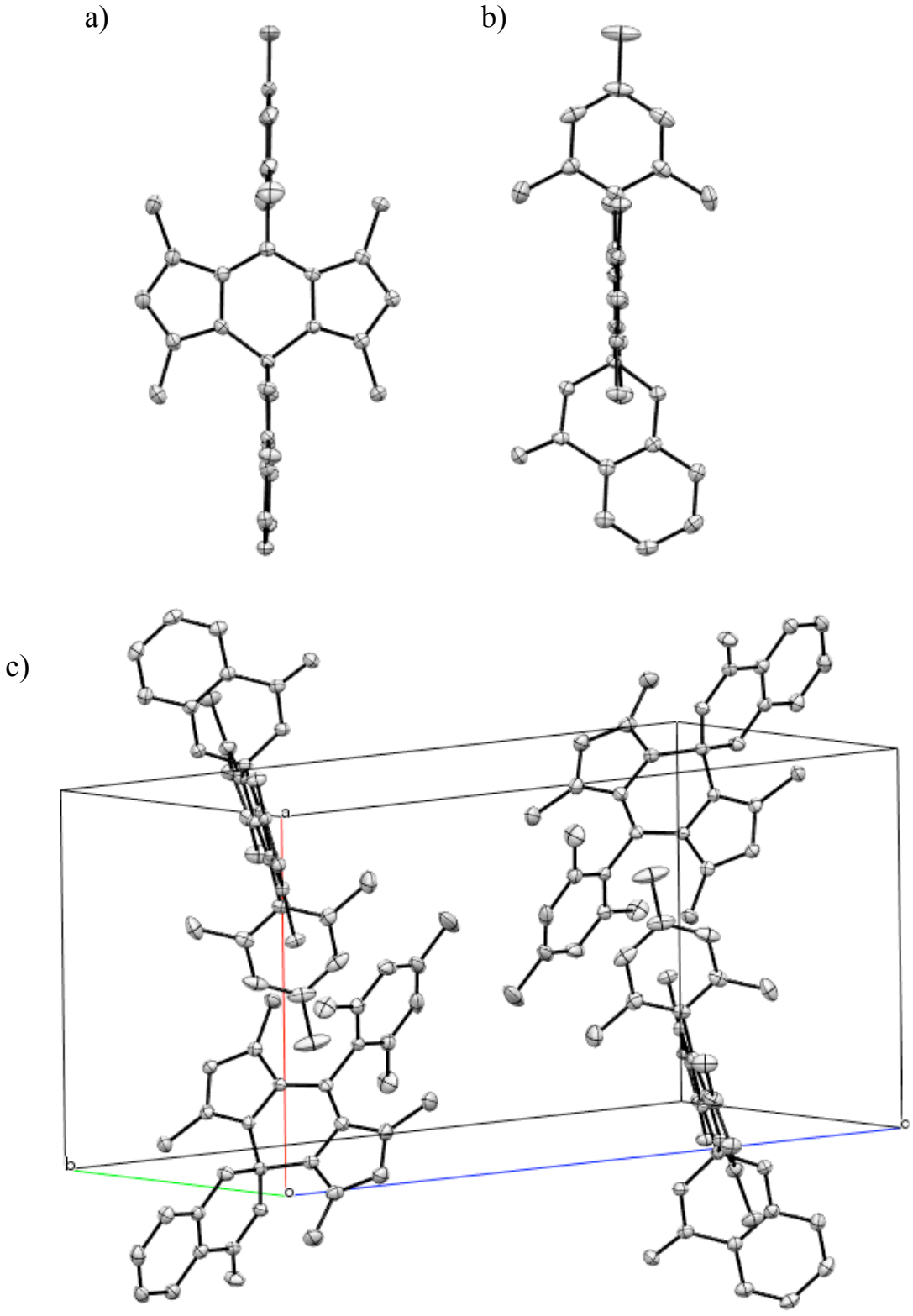

Compound **1h**. (a) Top view. (b) Side view. (c) Crystal packing diagram.

a)

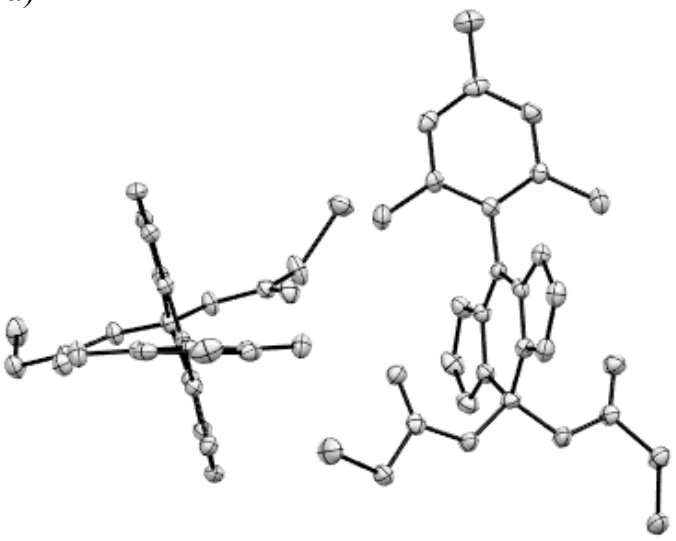

c)

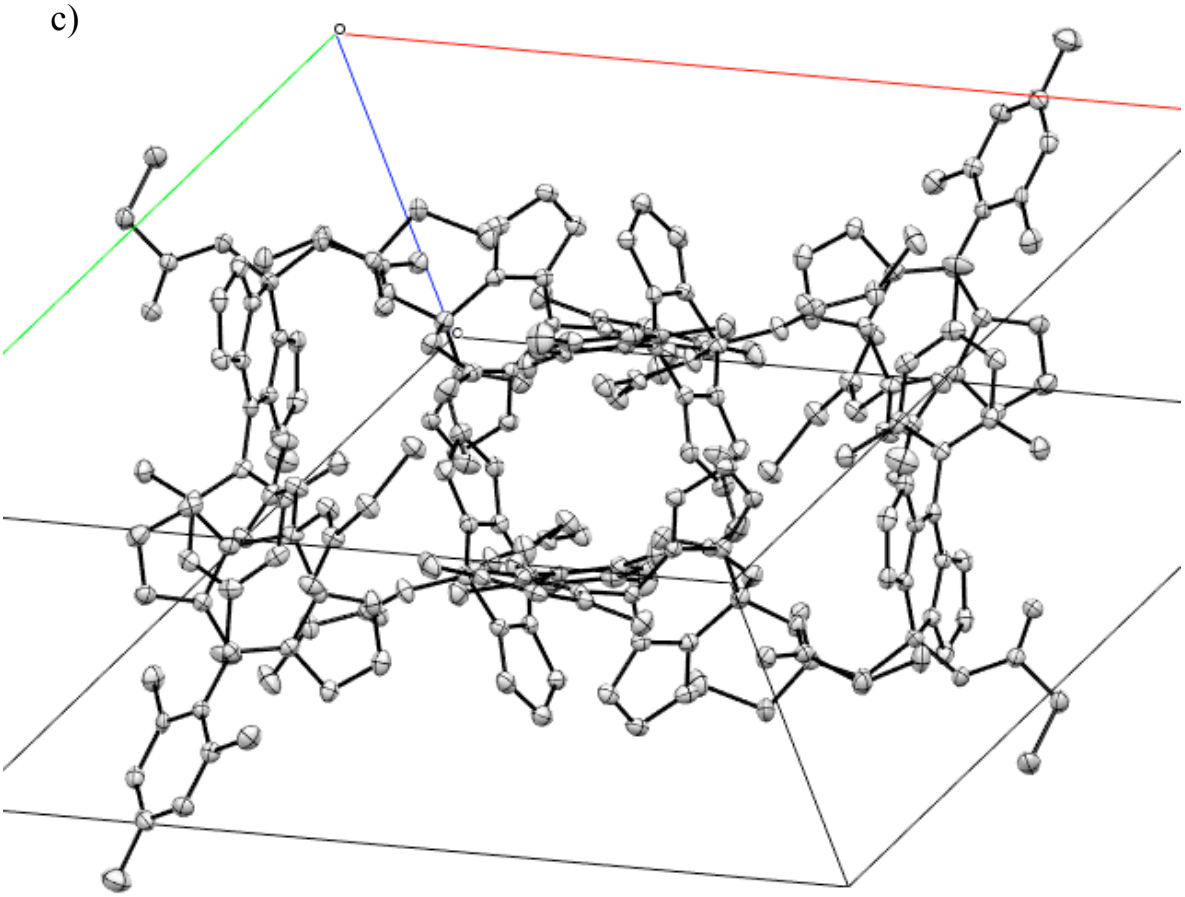

Compound **1j**. (a) Two independent molecules in the crystal cell. (b) Crystal packing diagram.

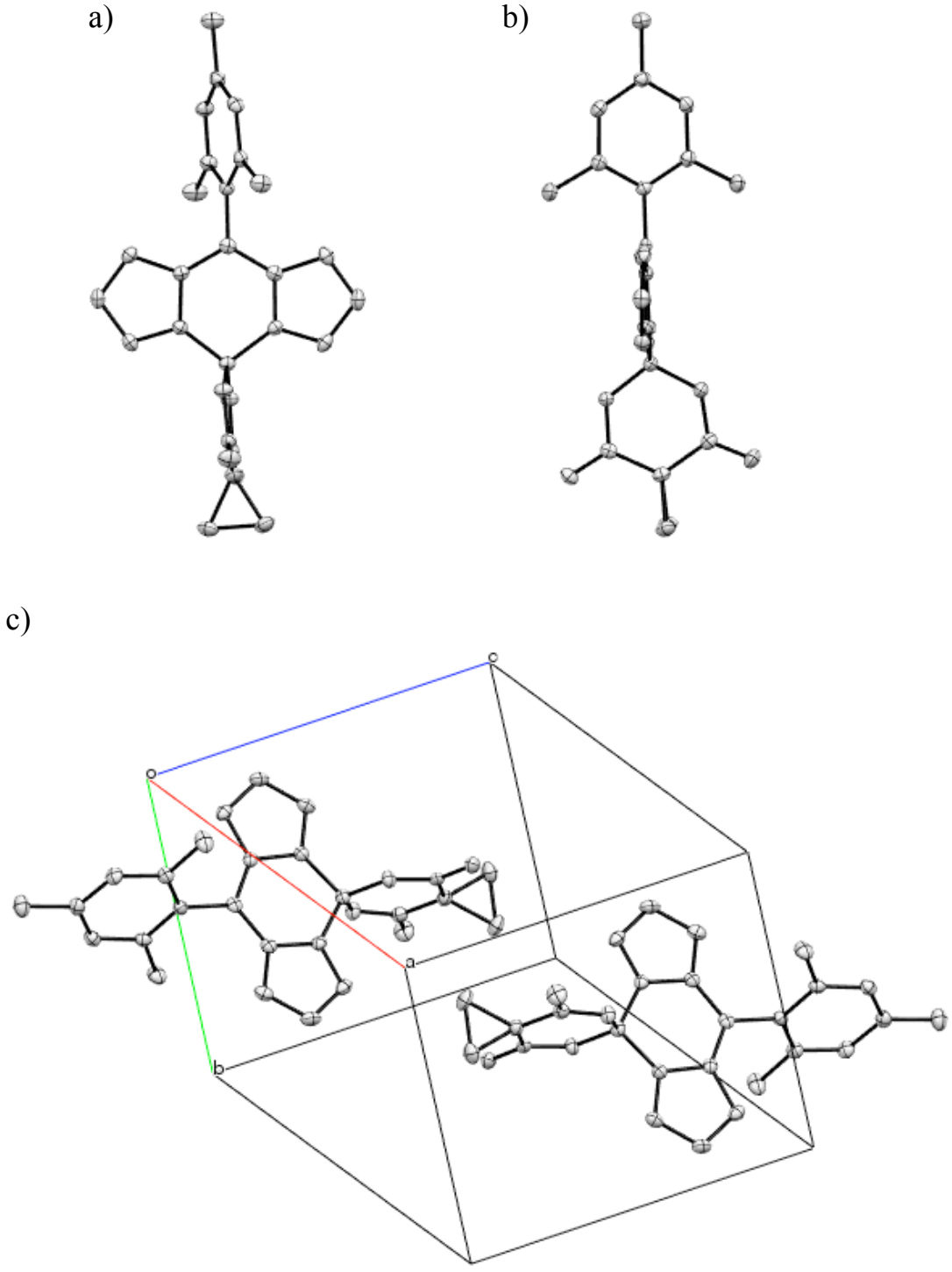

Compound **2b**. (a) Top view. (b) Side view. (c) Crystal packing diagram.

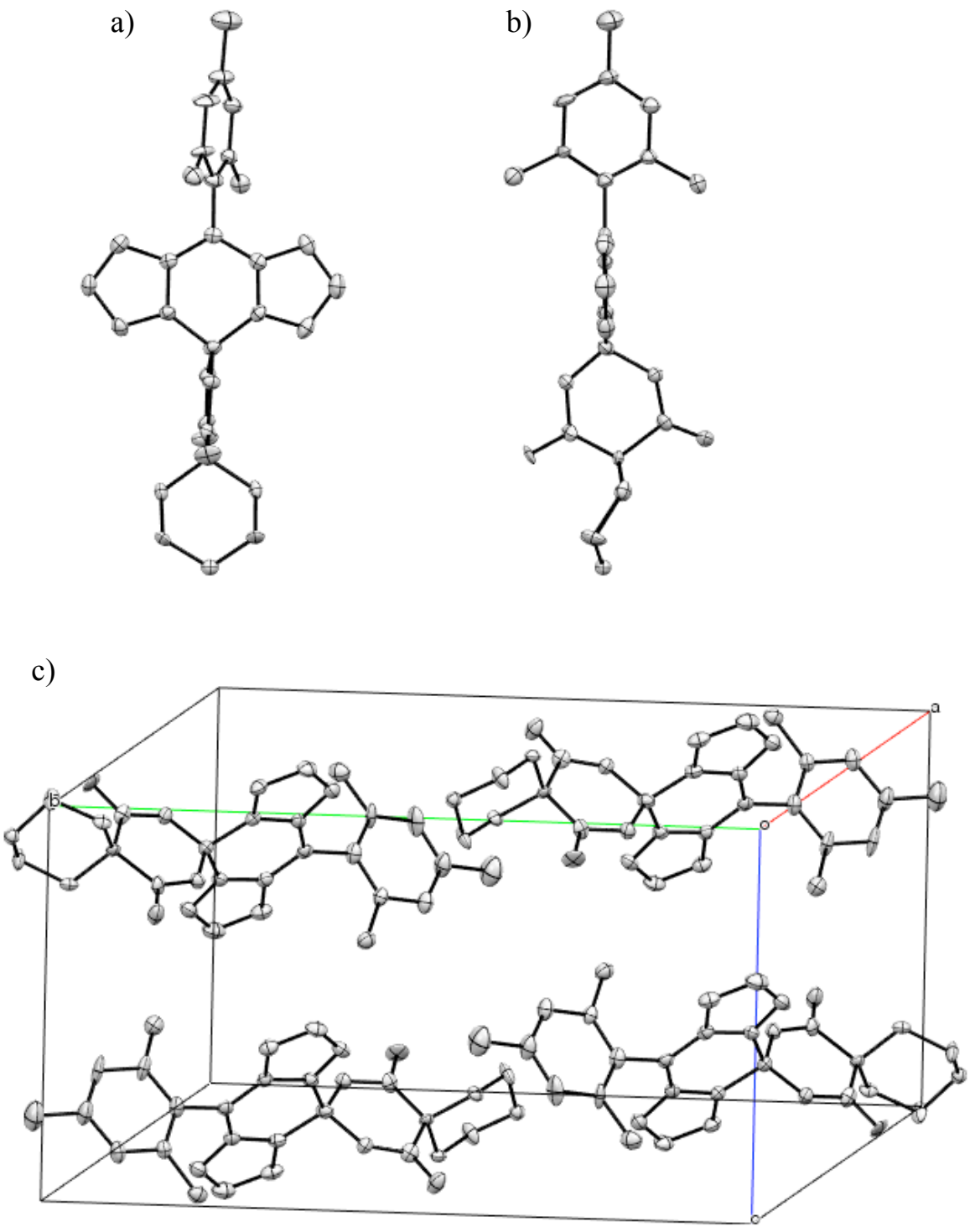

Compound **2e**. (a) Top view. (b) Side view. (c) Crystal packing diagram.

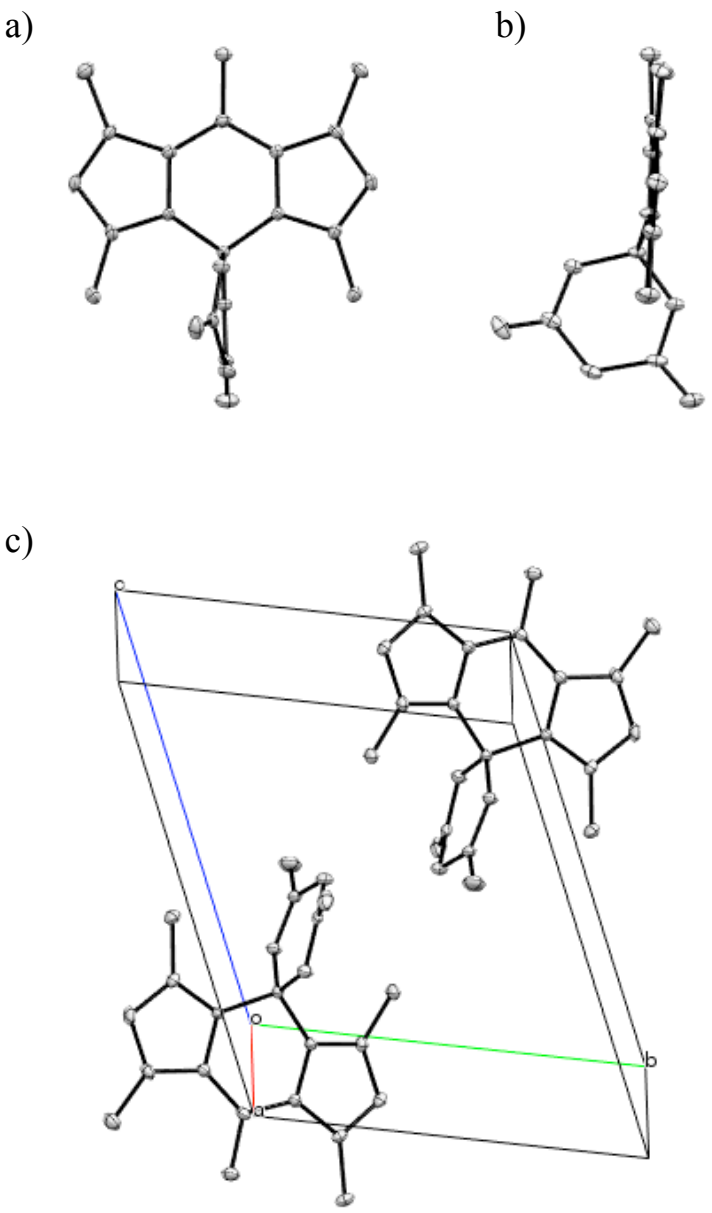

Compound **4a**. (a) Top view. (b) Side view. (c) Crystal packing diagram.

Table S1. Selected structural data for BODIPYs **1a-d**, **1h**, **2e**, **2e**, **2j**, and **4a** in the crystalline form.

	1a[a)]	**1b**	**1c**	**1d**	**1h**	**2b**	**2e**	**2j**[a)]	**4a**
$d_{B—N}$ (Å)	1.539(2) 1.547(2) 1.540(2) 1.541(2)	1.541(2) 1.545(1)	1.540(2) 1.545(2)	1.546(2) 1.549(3)	1.545(3) 1.555(2)	1.541(2) 1.548(2)	1.540(3) 1.550(3)	1.533(7) 1.542(7) 1.534(7) 1.540(7)	1.534(4) 1.539(3)
$d_{B—O}$ (Å)	1.467(2) 1.474(2) 1.467(2) 1.477(2)	1.467(1) 1.474(1)	1.469(2) 1.475(1)	1.466(3) 1.479(2)	1.452(3) 1.477(2)	1.461(2) 1.461(2)	1.412(4) 1.521(7)	1.474(6) 1.477(6) 1.474(6) 1.479(6)	1.464(3) 1.482(3)
$\Delta(BN_2C_3)_{mean}$[b)]	0.013 0.048	0.022	0.011	0.010	0.016	0.025	0.007	0.015 0.018	0.064
$\Delta(BN_2C_3)_{max}$[c)]	0.023 0.085	0.043	0.021	0.017	0.029	0.048	0.011	0.026 0.033	0.126
<(NBN)[d)]	107.0(1)° 107.5(1)°	107.2(9)°	107.2(1)°	112.0(2)°	106.5(1)°	105.6(1)°	105.6(2)°	107.3(4)° 106.1(4)°	107.1(2)
<(OBO)[e)]	113.2(1)° 113.4(1)°	113.1(9)°	112.3(1)°	106.7(2)°	113.6(2)°	114.0(1)°	109.8(4)°	101.9(4)° 101.3(4)°	113.4(2)
<(C(O_2)CC(O_2))[f)]	117.9(1)° 117.8(2)°	120.0(9)°	115.9(1)°	115.1(2)°	–	120.4(1)°	114.5(4)°	–	117.4(2)
<(BDP/BO_2C_3)[g)]	82.3° 86.7°	89.4°	85.5°	84.3°	89.2°	87.7°	88.2°	89.7°[h)] 89.0°[h)]	85.9°
<(BDP/Mes)[i)]	88.4°	79.6°	88.2°	87.7°	88.8°	70.0°	72.7°	80.7°	–

[a)]Measurements for two independent molecules in the unit cell; [b)]Mean deviation distance for the atoms of the BN_2C_3 central ring with respect to the least squares mean plane of the ring; [c)]Maximum deviation distance for the atoms of the BN_2C_3 central ring with respect to the least squares mean plane of the ring; [d)]N—B—N bond angle; [e)]O—B—O bond angle; [f)]O_2C—C—CO_2 bond angle; [g)]Dihedral angle between the least squares mean planes of the boradiazaindacene (C_9BN_2) system and the dioxaborinane (BO_2C_3) ring; [h)]Dihedral angle between the least squares mean plane of the boradiazaindacene (C_9BN_2) system and the plane of the O—B—O group; [i)]Dihedral angle between the least squares mean plane of the boradiazaindacene (C_9BN_2) system and the mesityl ring.

4. ^{1}H and ^{13}C NMR spectra of the new dyes.

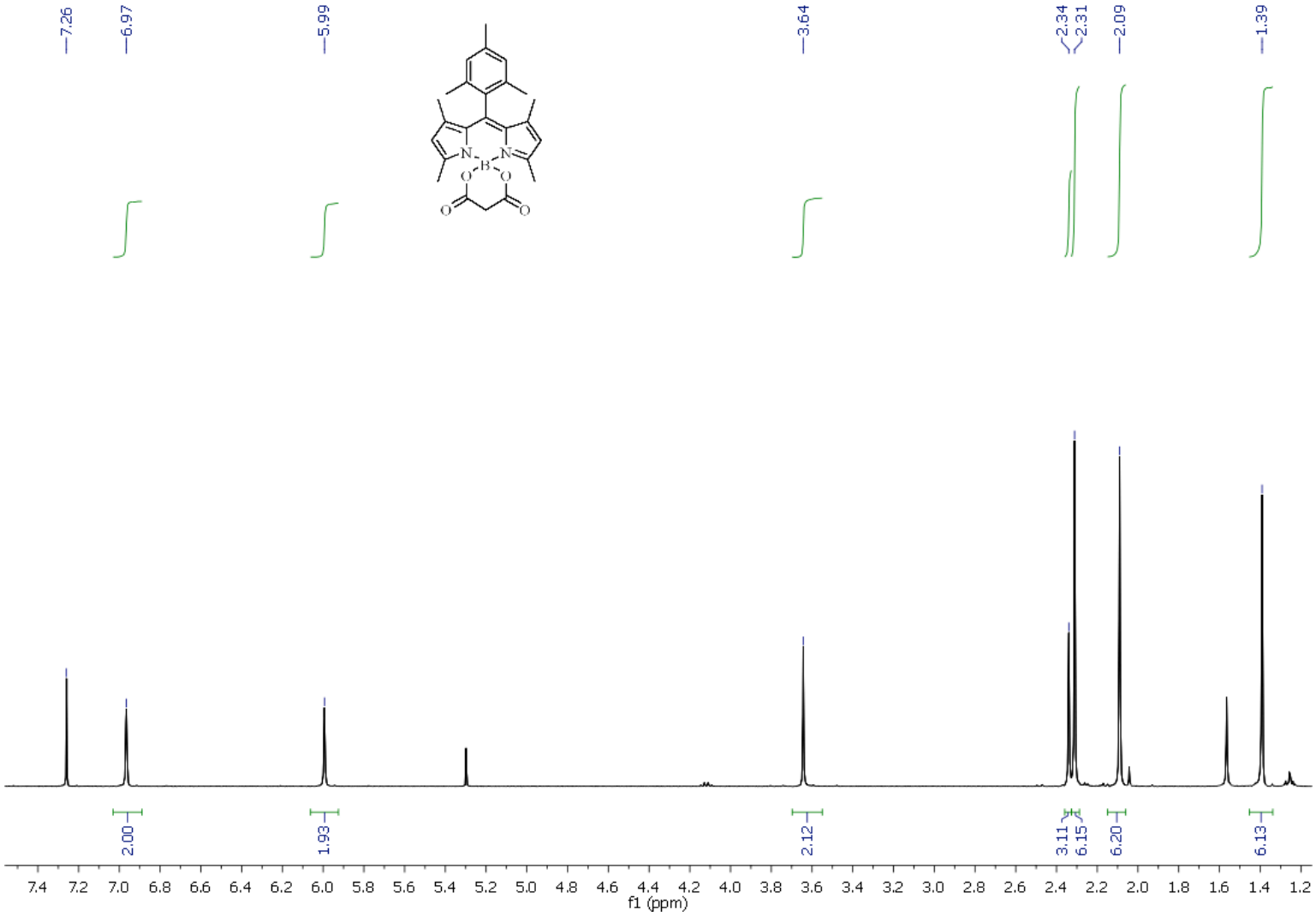

^{1}H NMR (400 MHz, $CDCl_3$) spectrum of compound **1a**

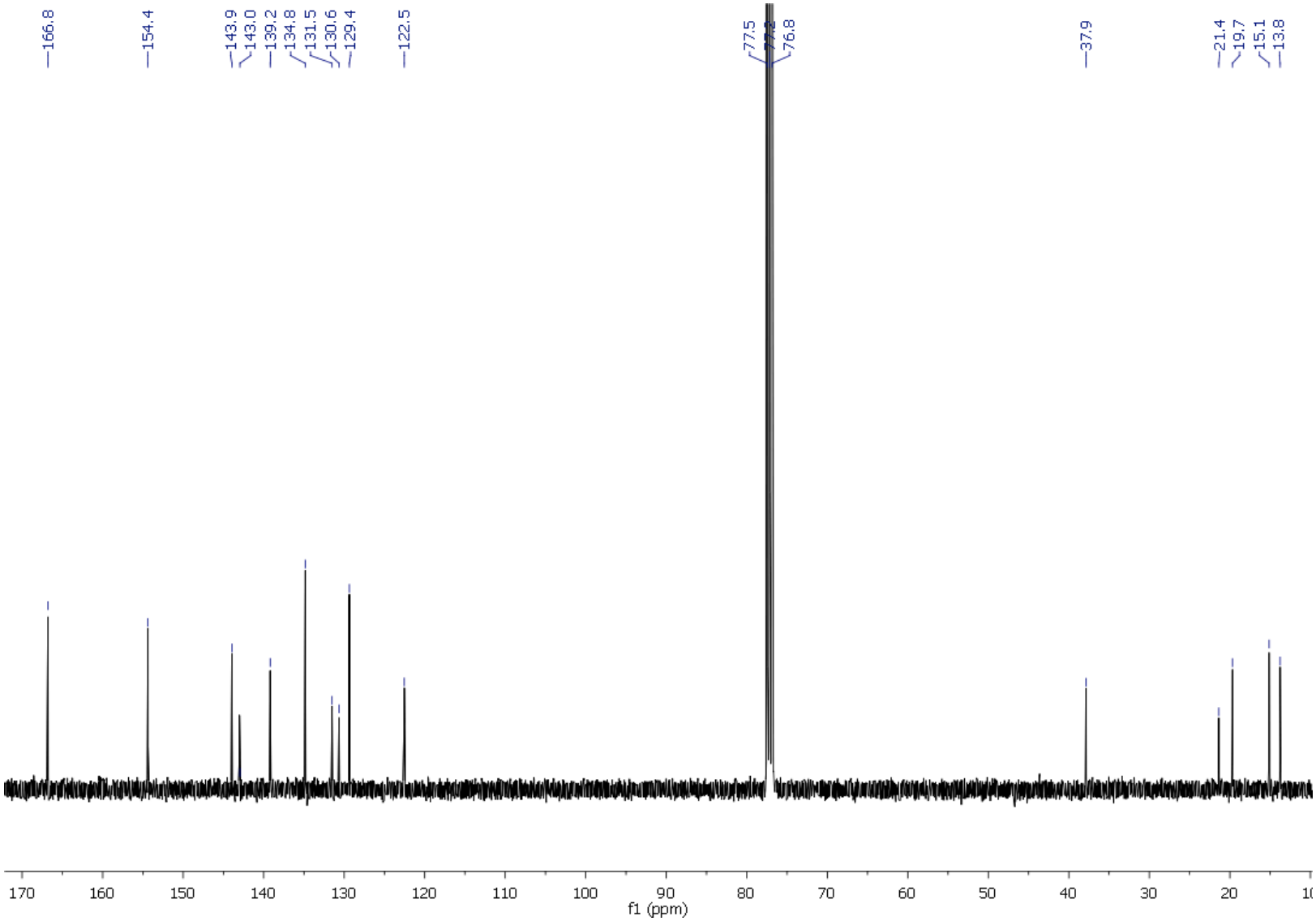

^{13}C NMR (100 MHz, $CDCl_3$) spectrum of compound **1a**

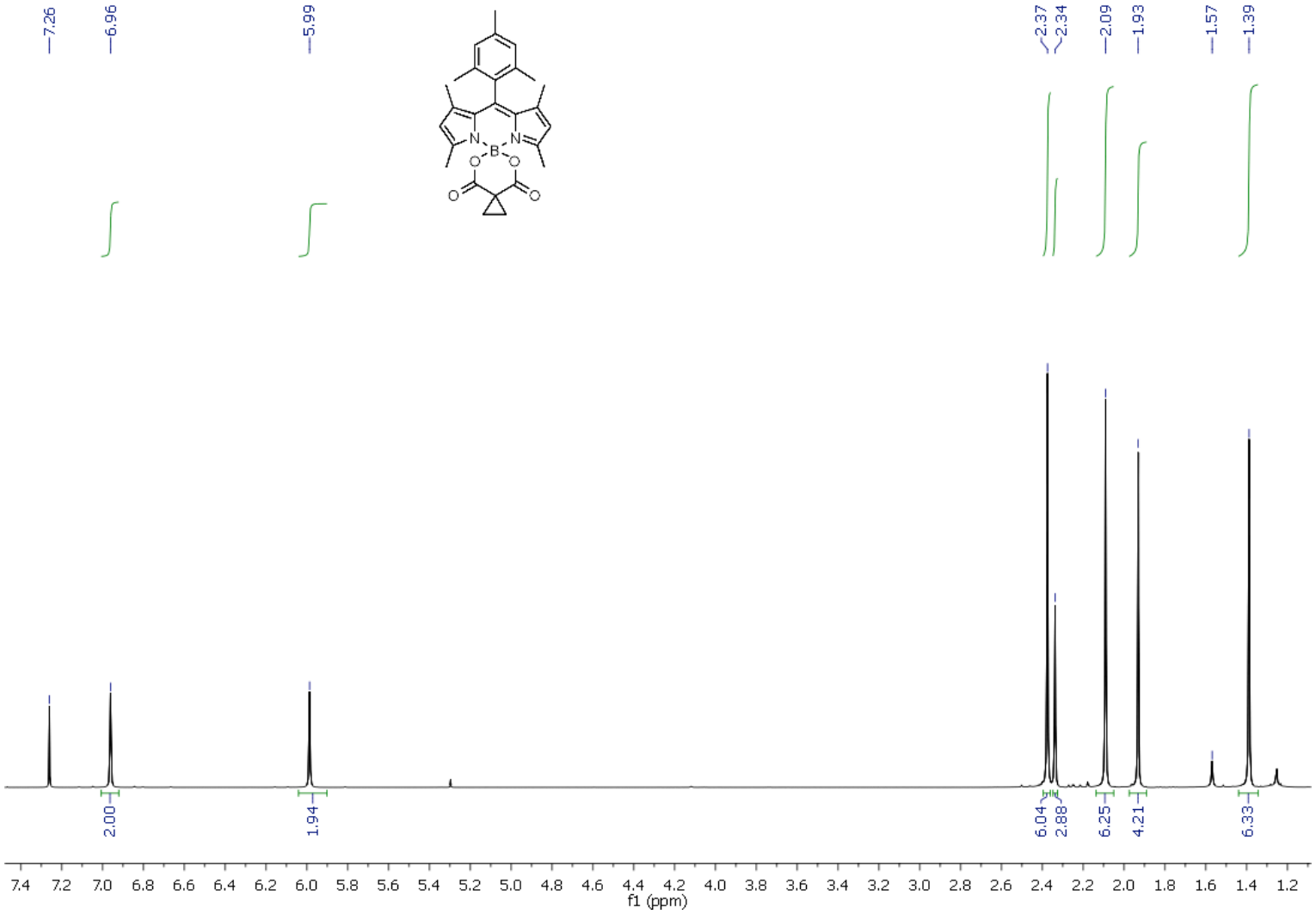

^{1}H NMR (500 MHz, $CDCl_3$) spectrum of compound **1b**

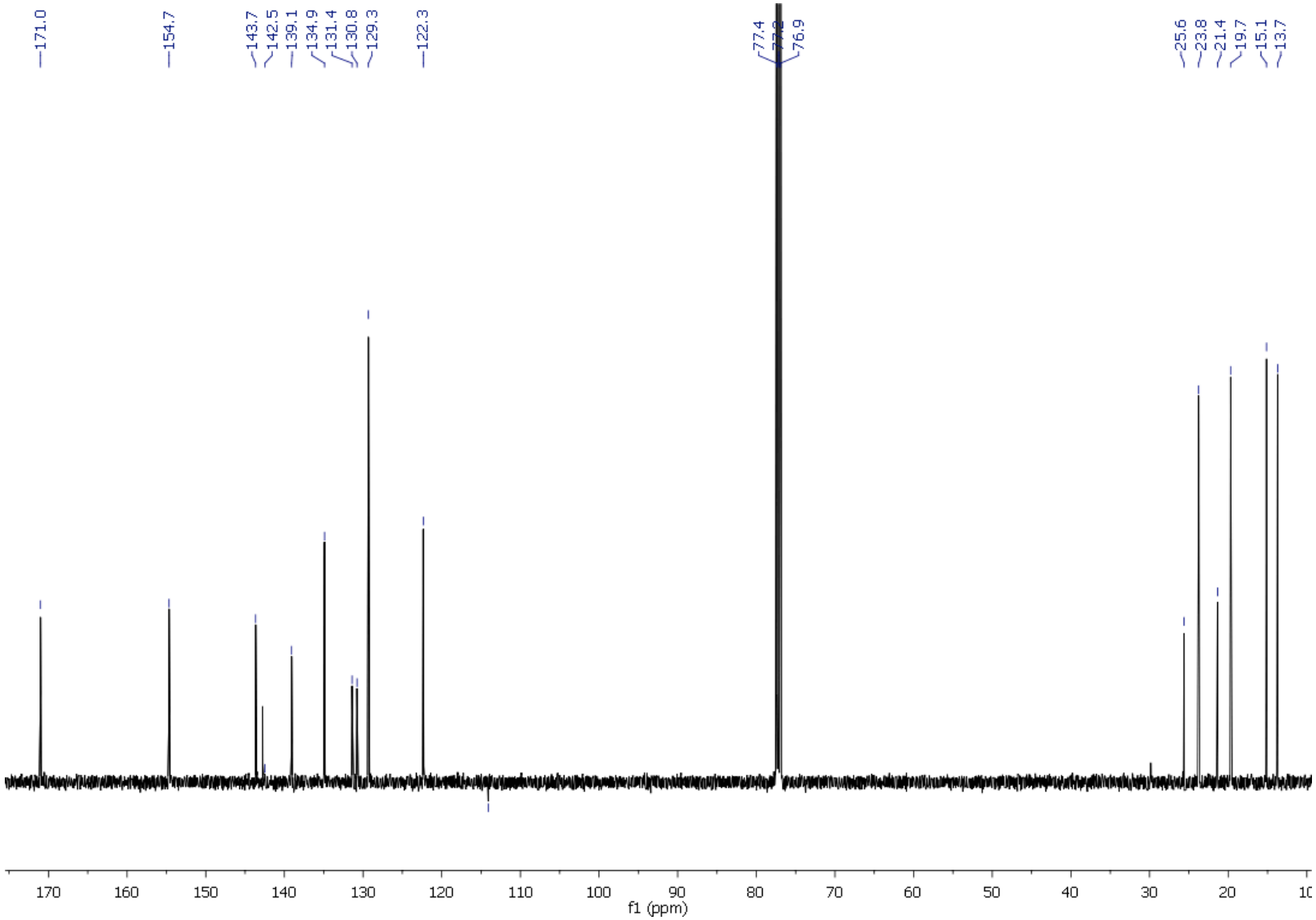

^{13}C NMR (125 MHz, $CDCl_3$) spectrum of compound **1b**

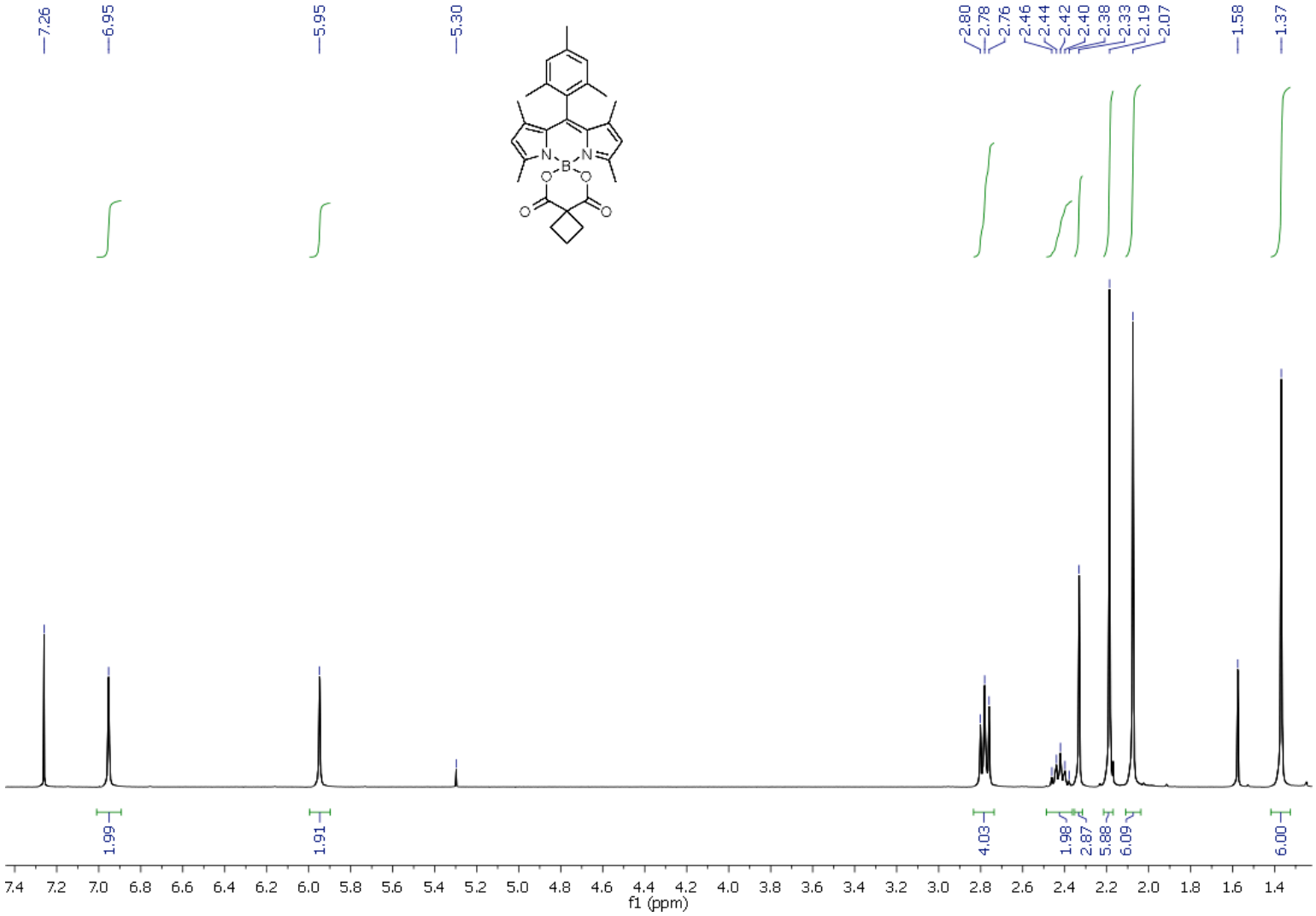

^{1}H NMR (400 MHz, $CDCl_3$) spectrum of compound **1c**

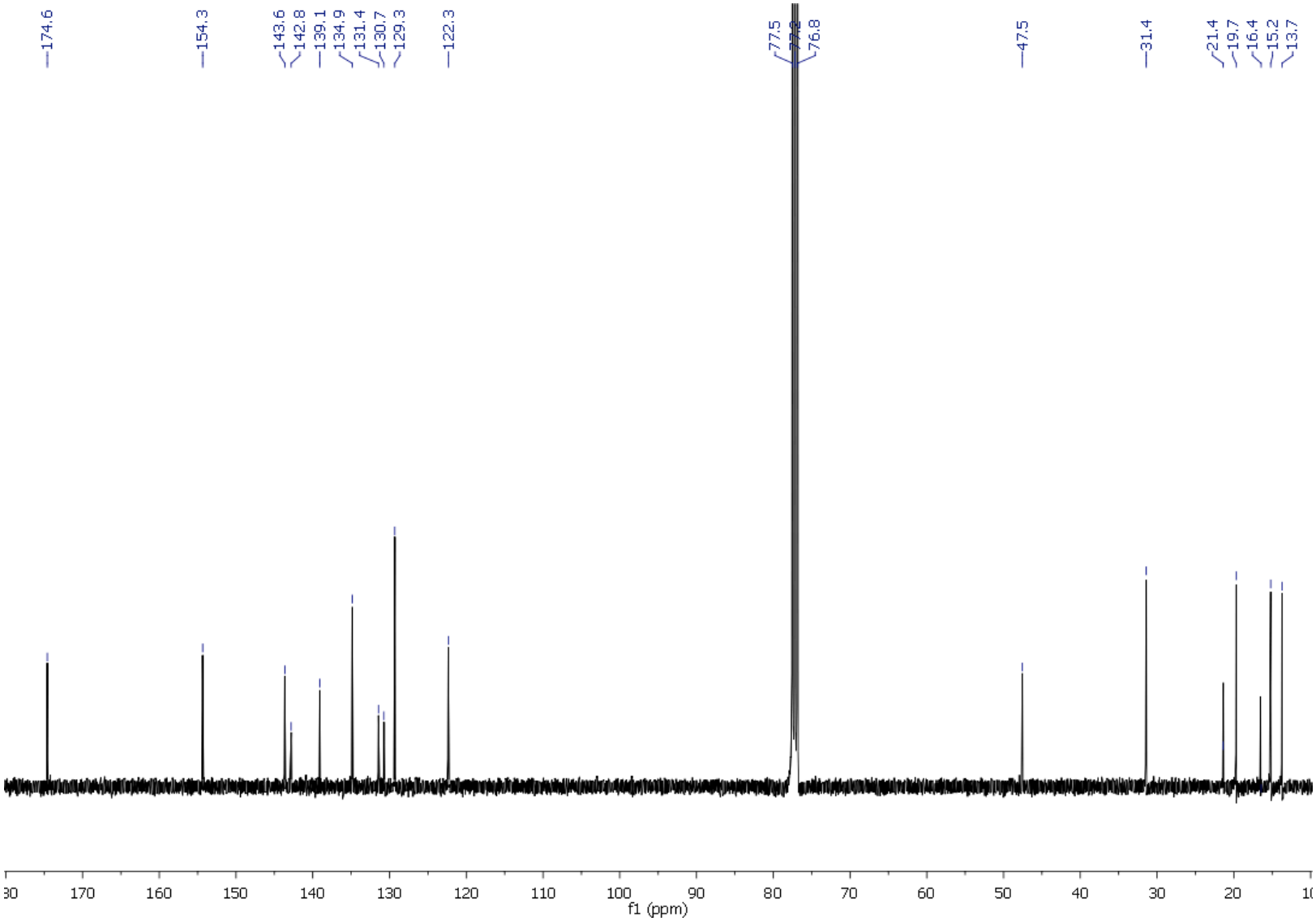

^{13}C NMR (100 MHz, $CDCl_3$) spectrum of compound **1c**

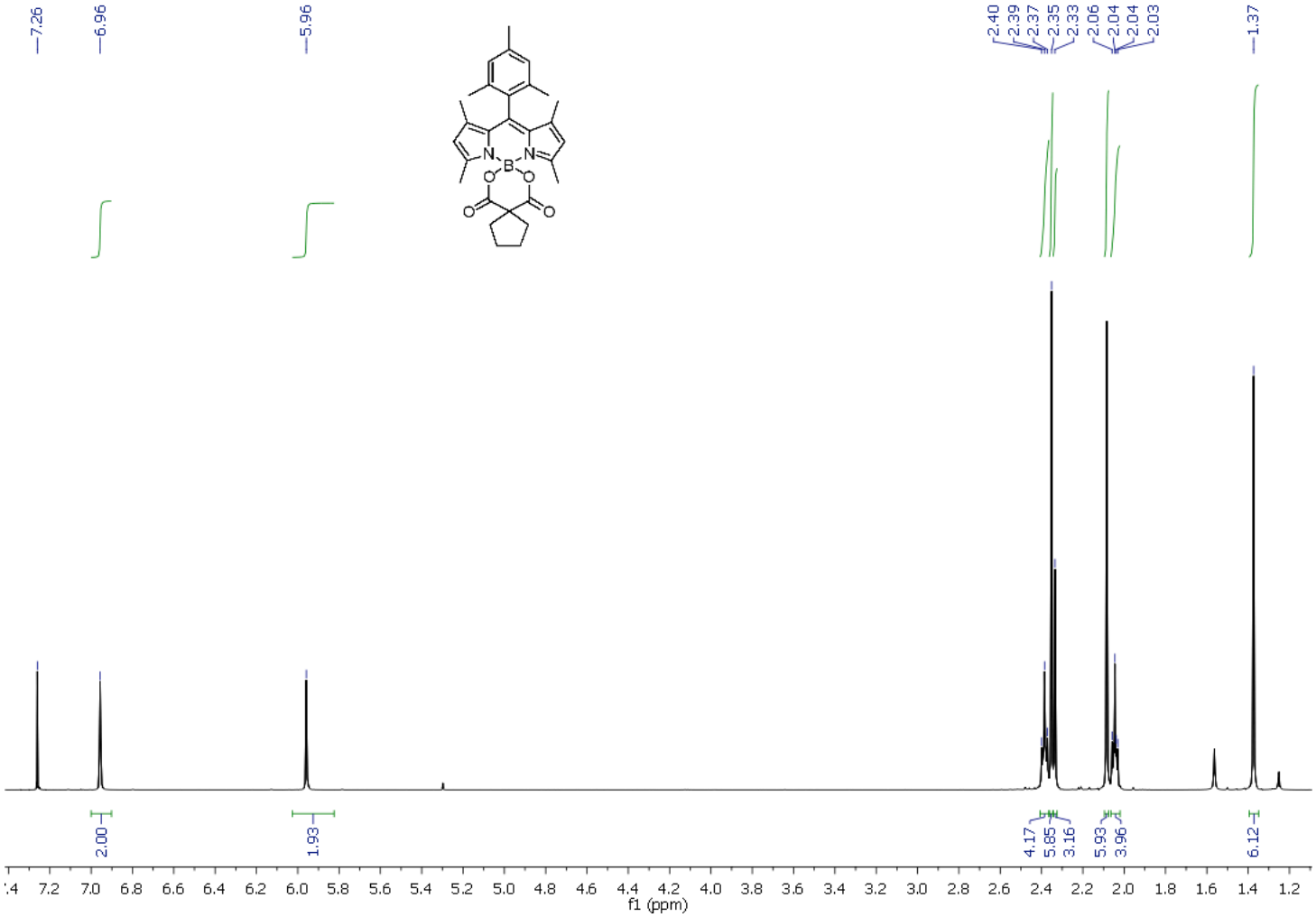

^{1}H NMR (500 MHz, $CDCl_3$) spectrum of compound **1d**

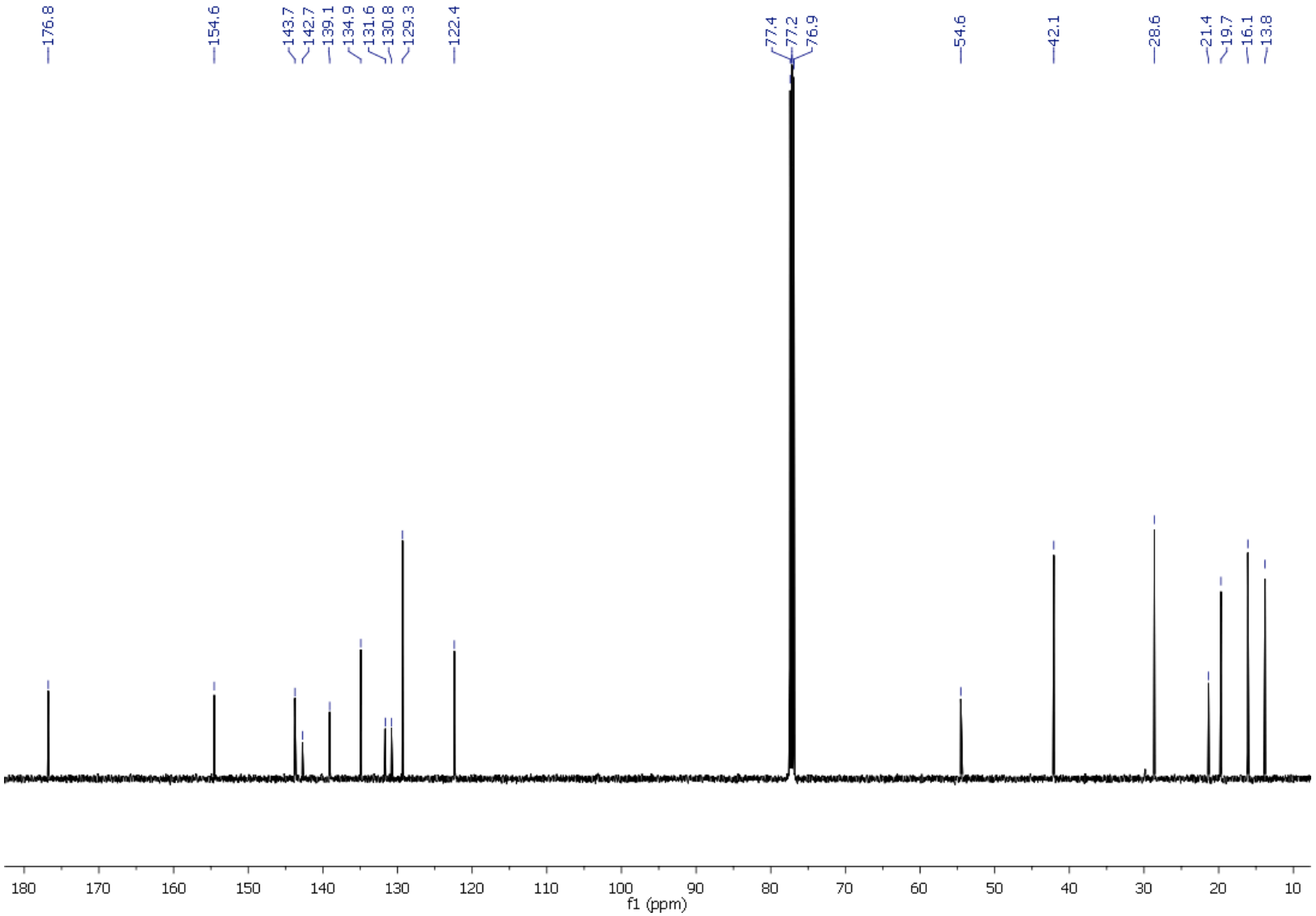

^{13}C NMR (125 MHz, $CDCl_3$) spectrum of compound **1d**

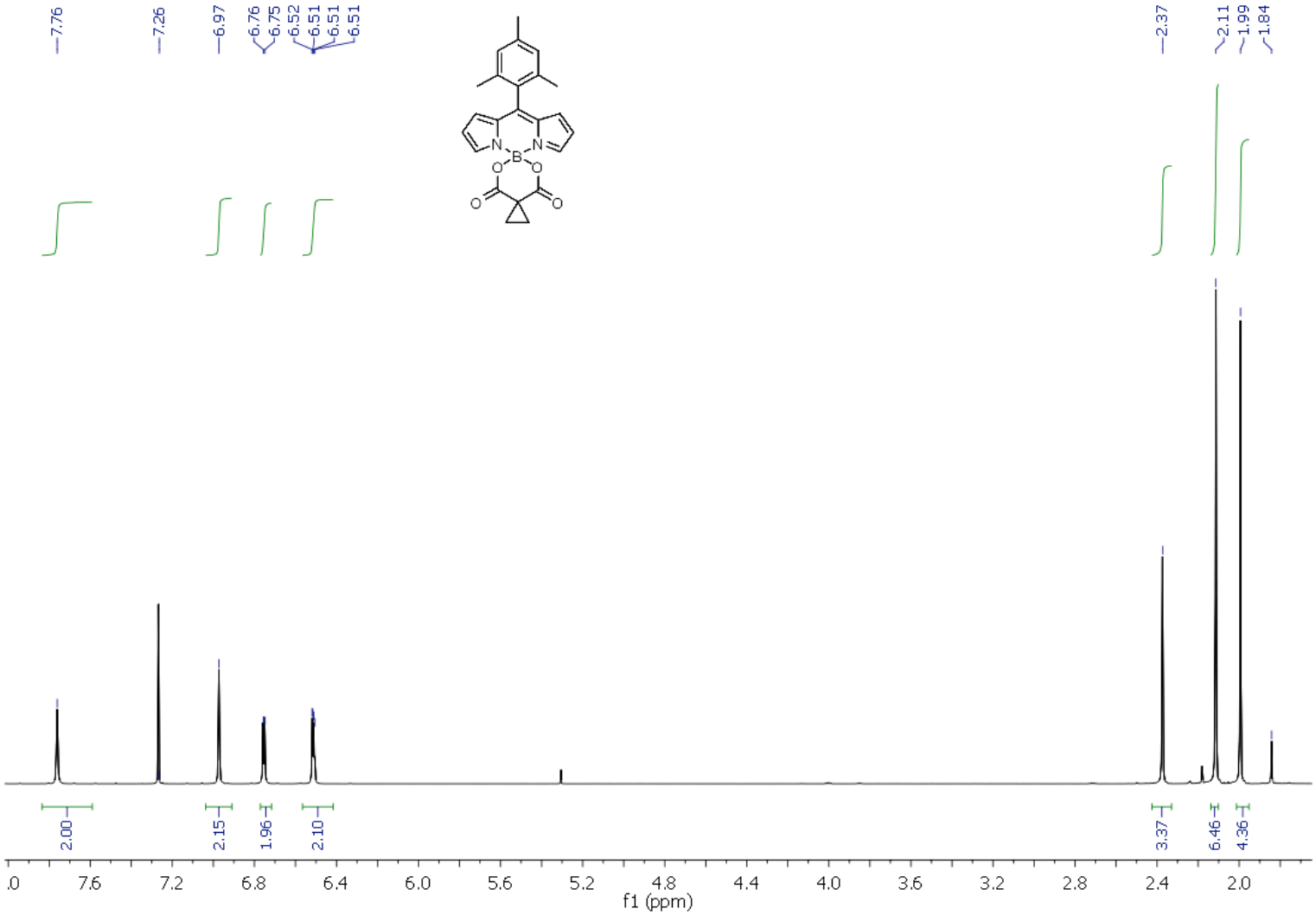

^{1}H NMR (500 MHz, $CDCl_3$) spectrum of compound **2b**

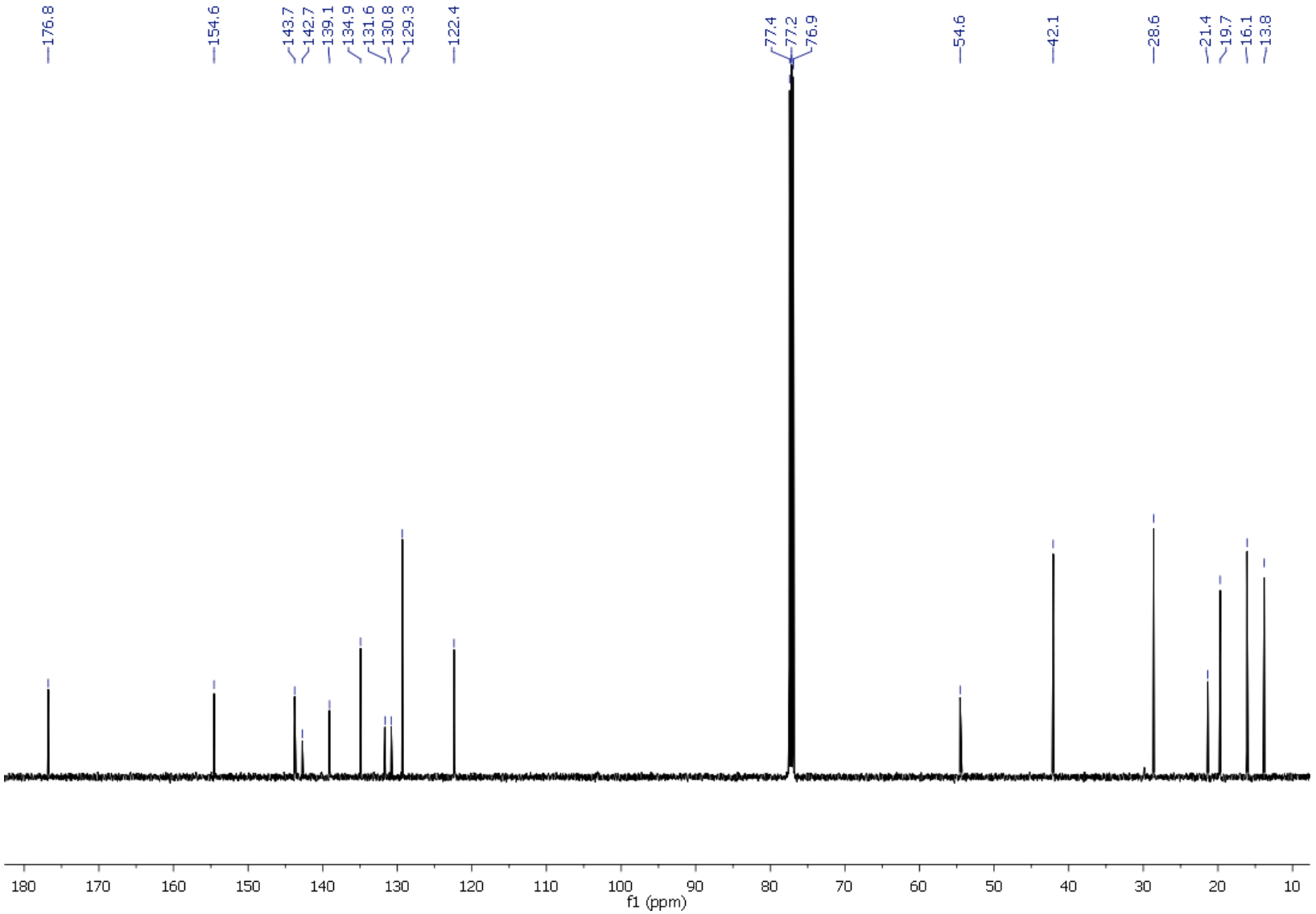

^{13}C NMR (125 MHz, $CDCl_3$) spectrum of compound **2b**

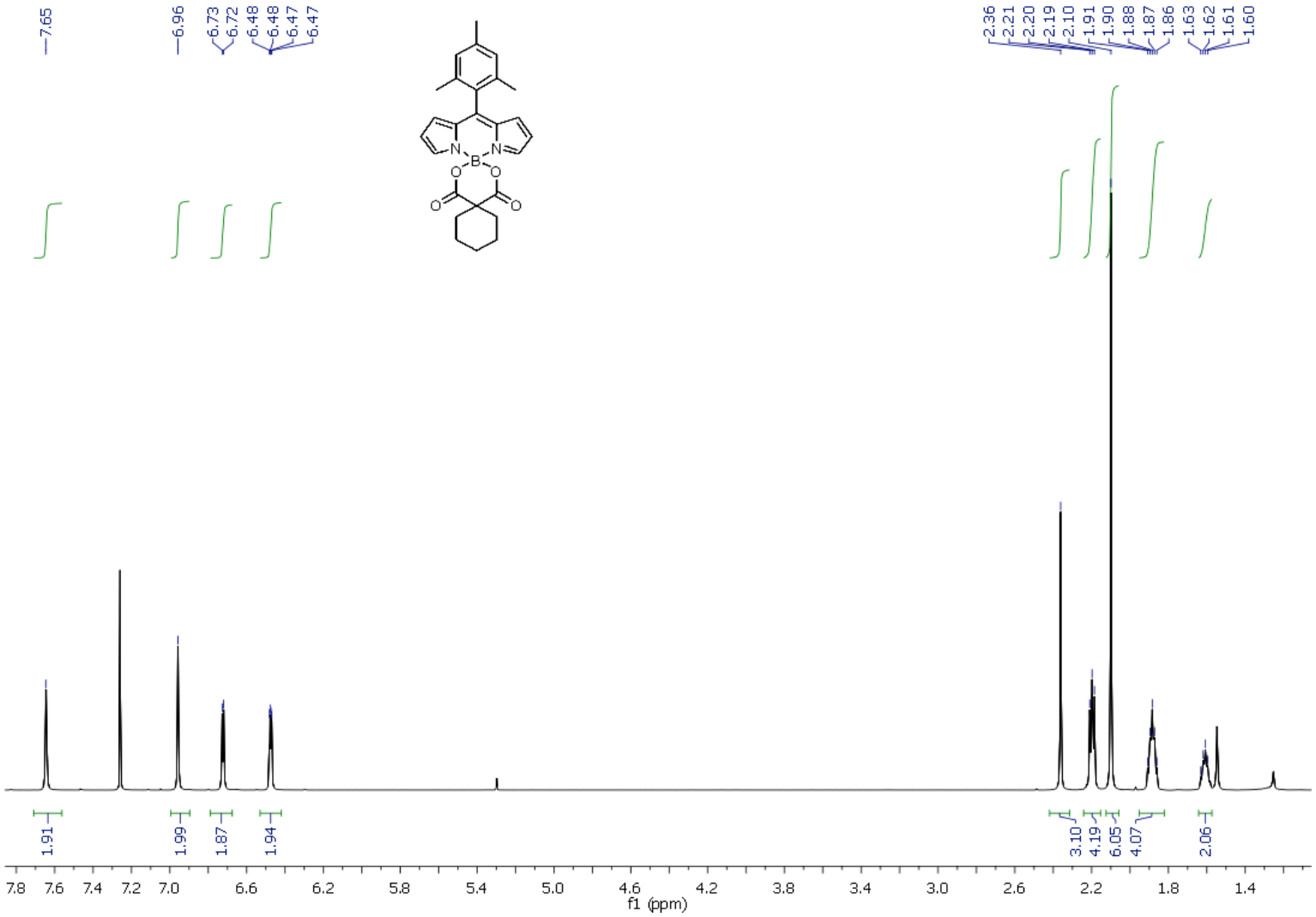

^{1}H NMR (500 MHz, $CDCl_3$) spectrum of compound **2e**

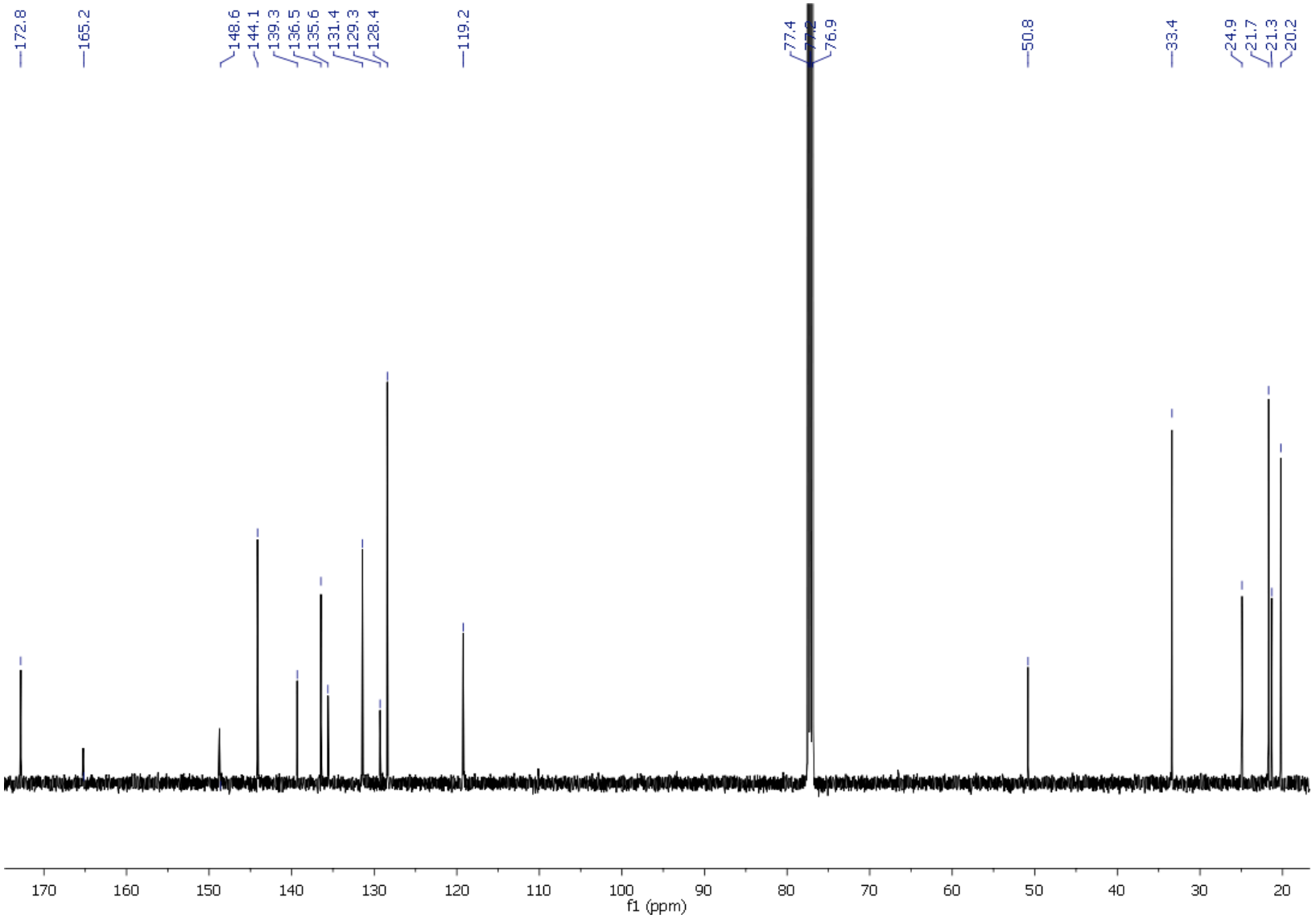

^{13}C NMR (125 MHz, $CDCl_3$) spectrum of compound **2e**

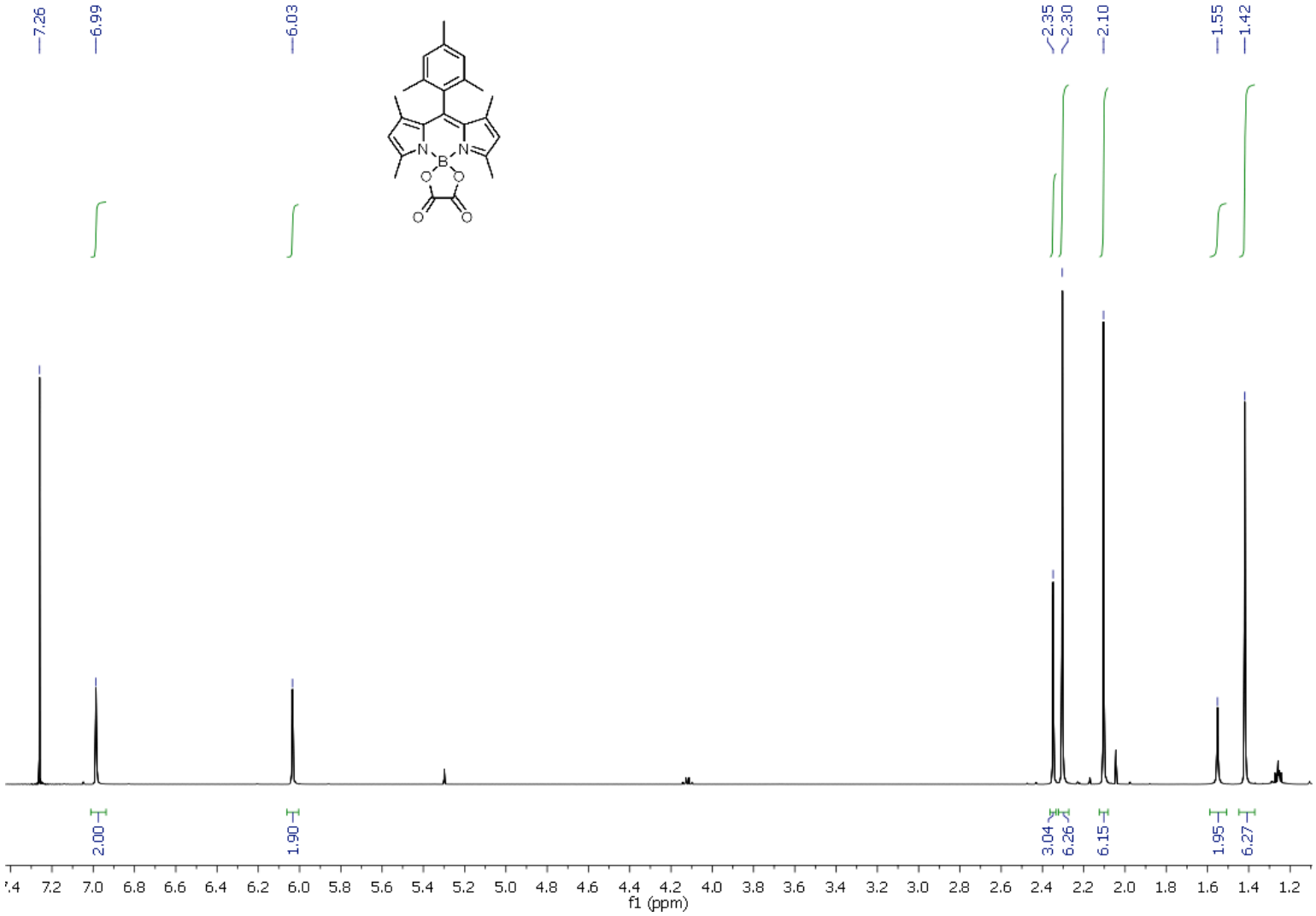

^{1}H NMR (500 MHz, $CDCl_3$) spectrum of compound **1g**

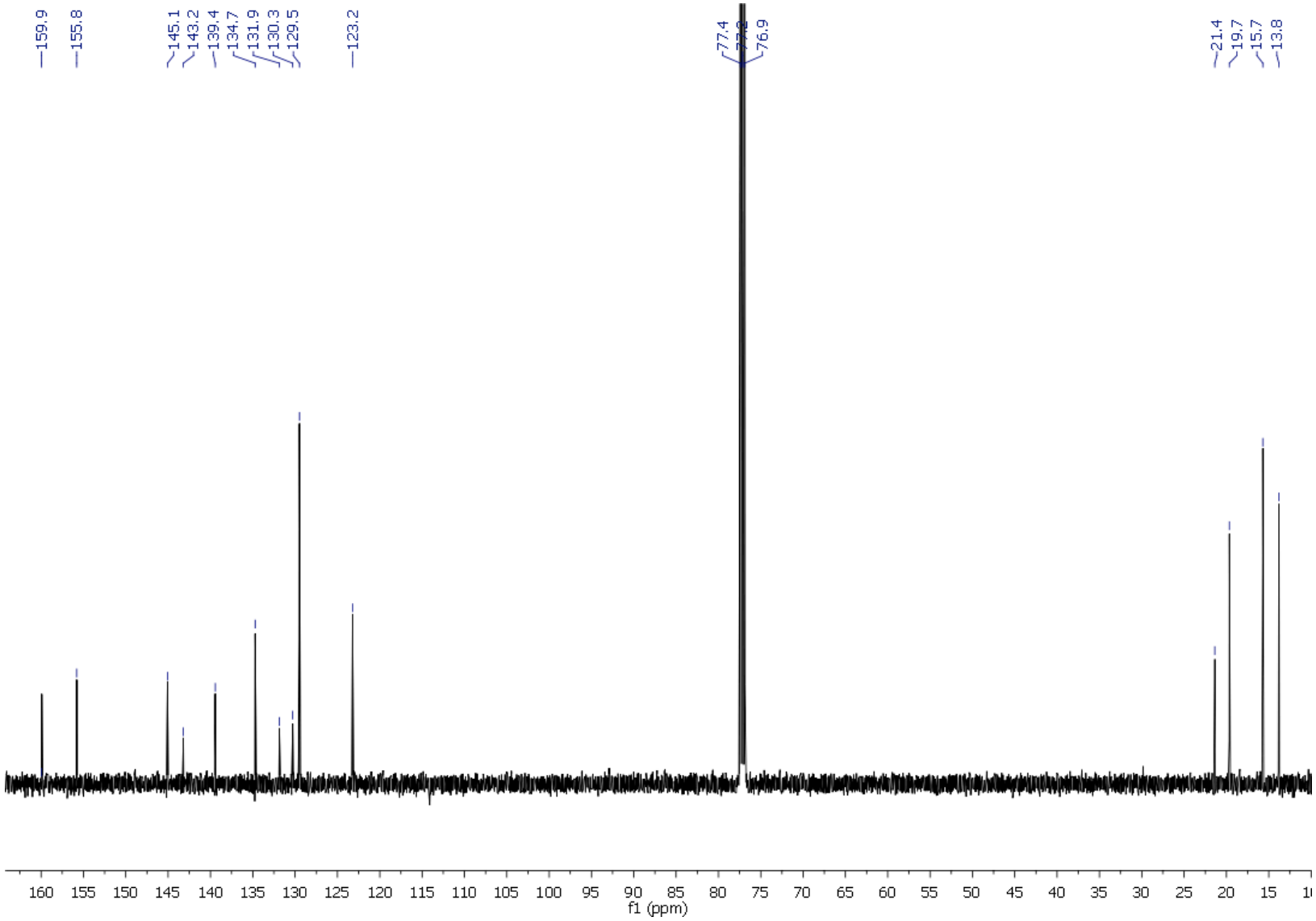

^{13}C NMR (125 MHz, $CDCl_3$) spectrum of compound **1g**

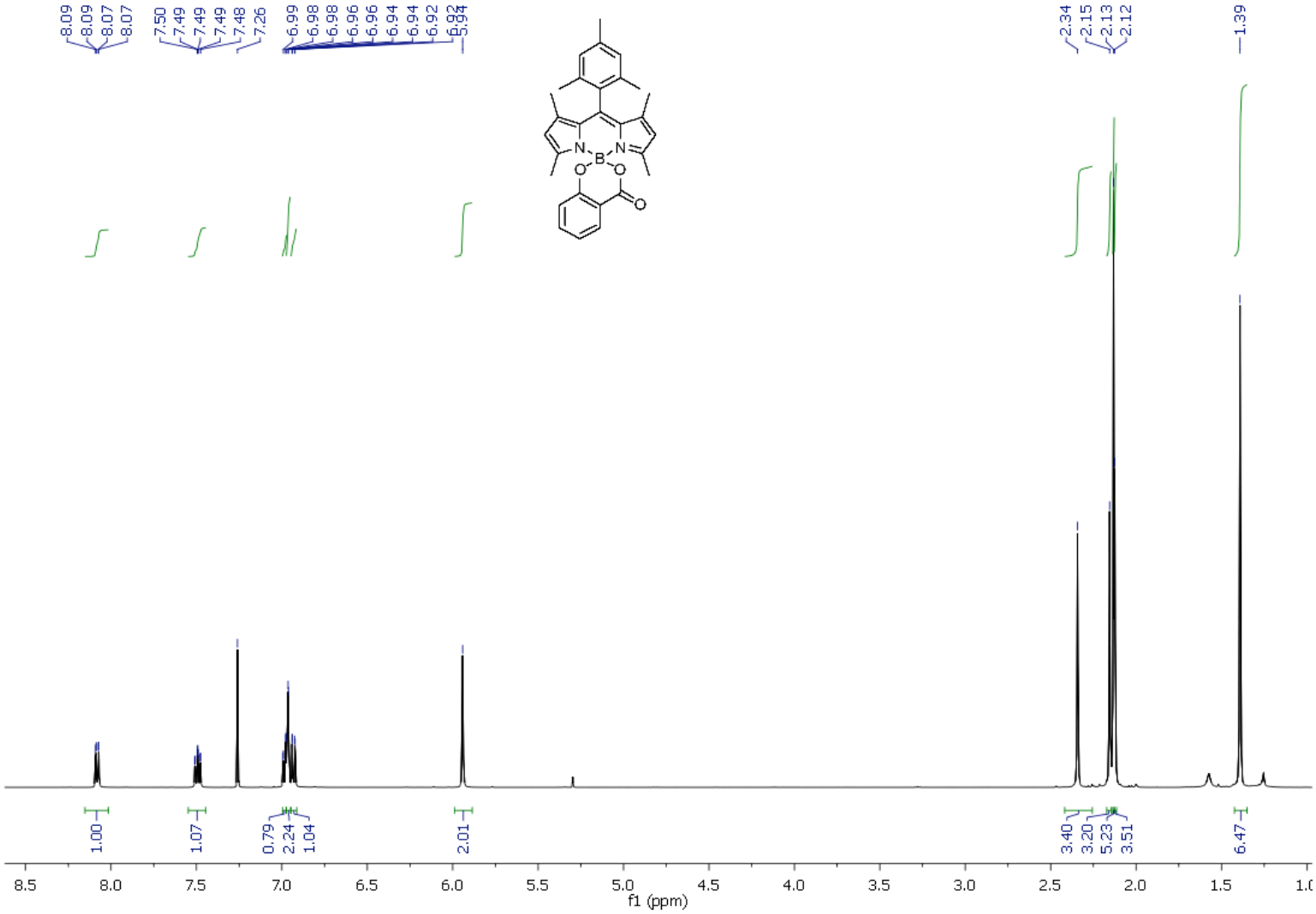

^{1}HNMR (500 MHz, $CDCl_3$) spectrum of compound **1h**

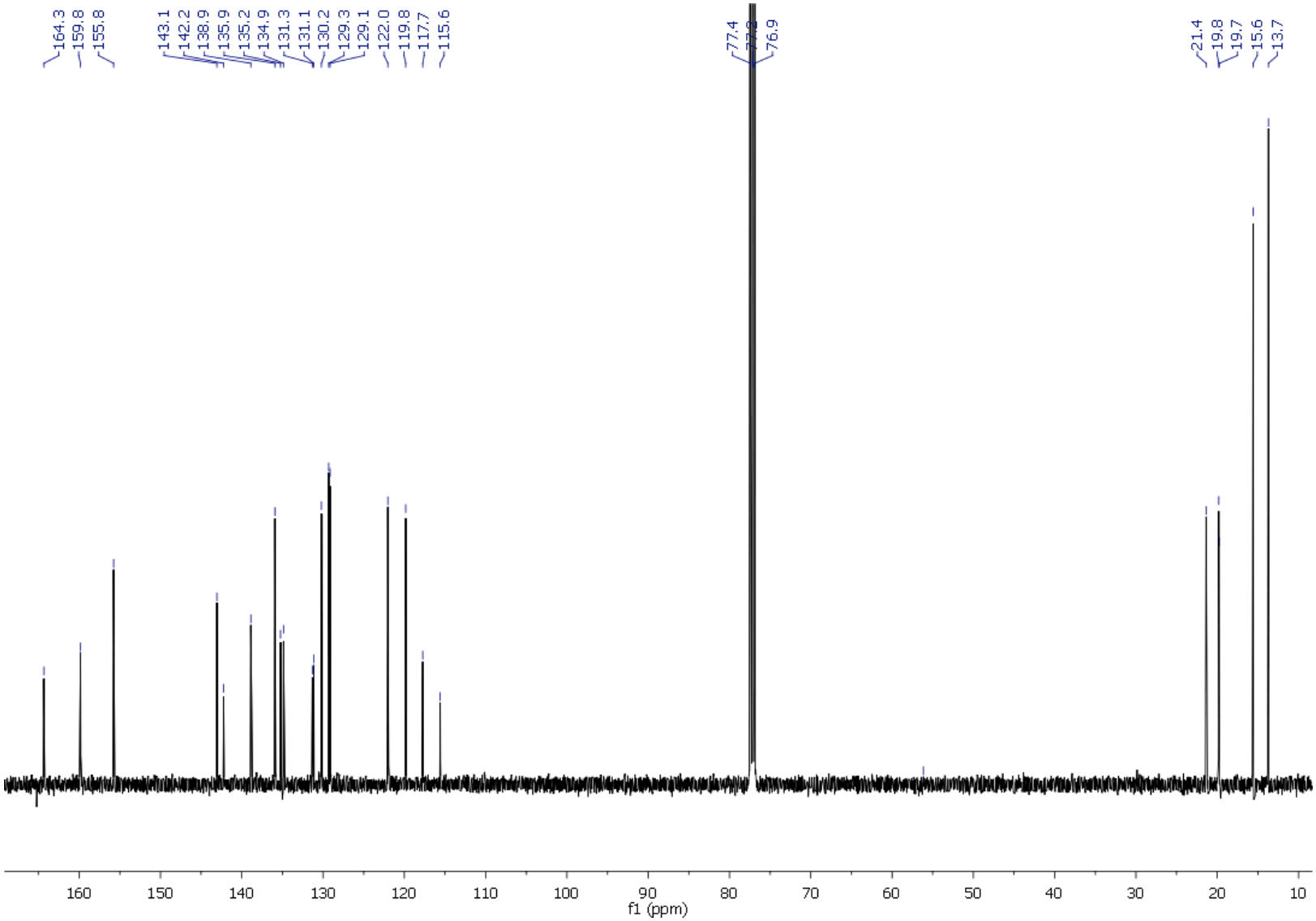

^{13}C NMR (125 MHz, $CDCl_3$) spectrum of compound **1h**

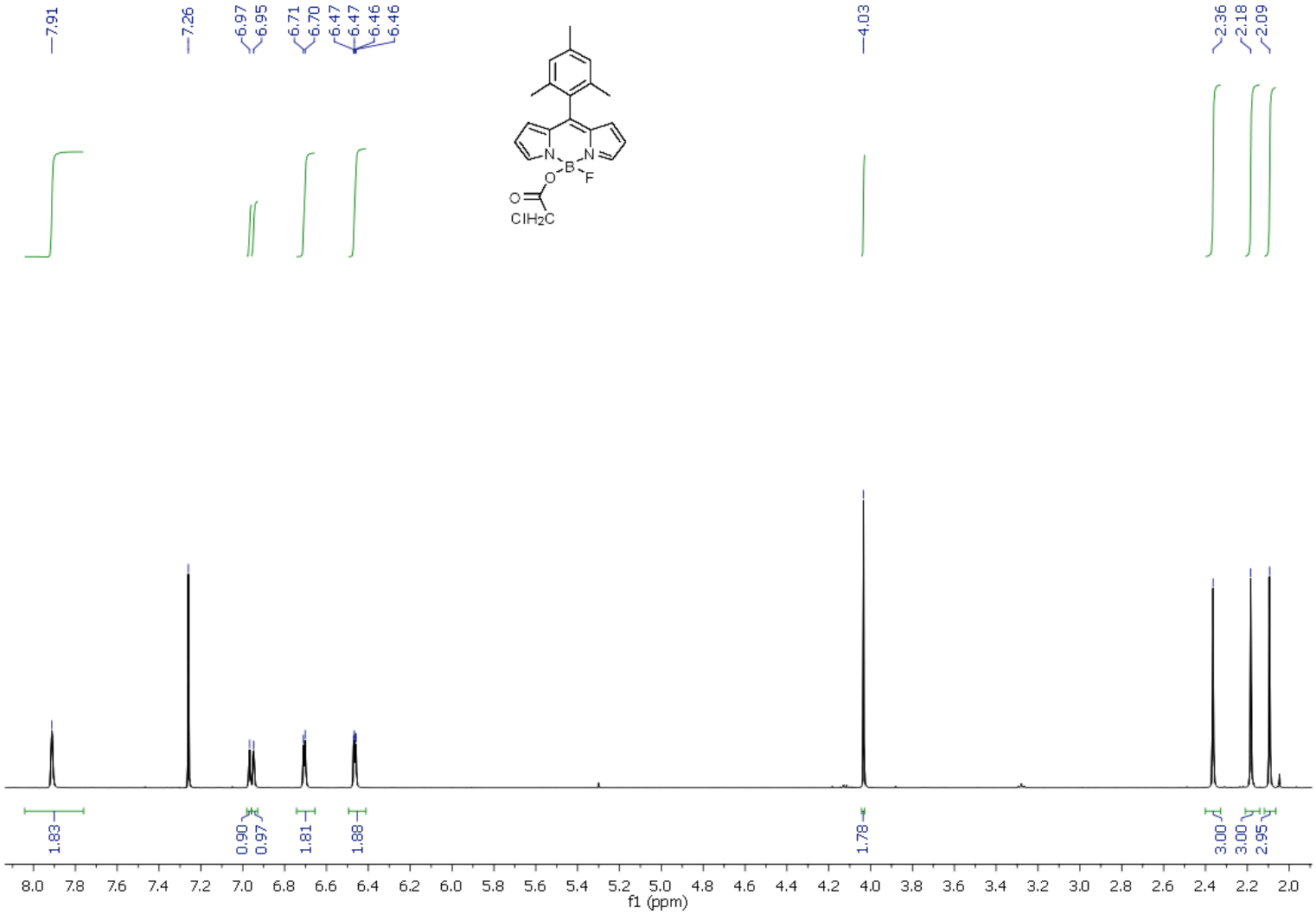

^{1}H NMR (500 MHz, $CDCl_3$) spectrum of compound **2i**

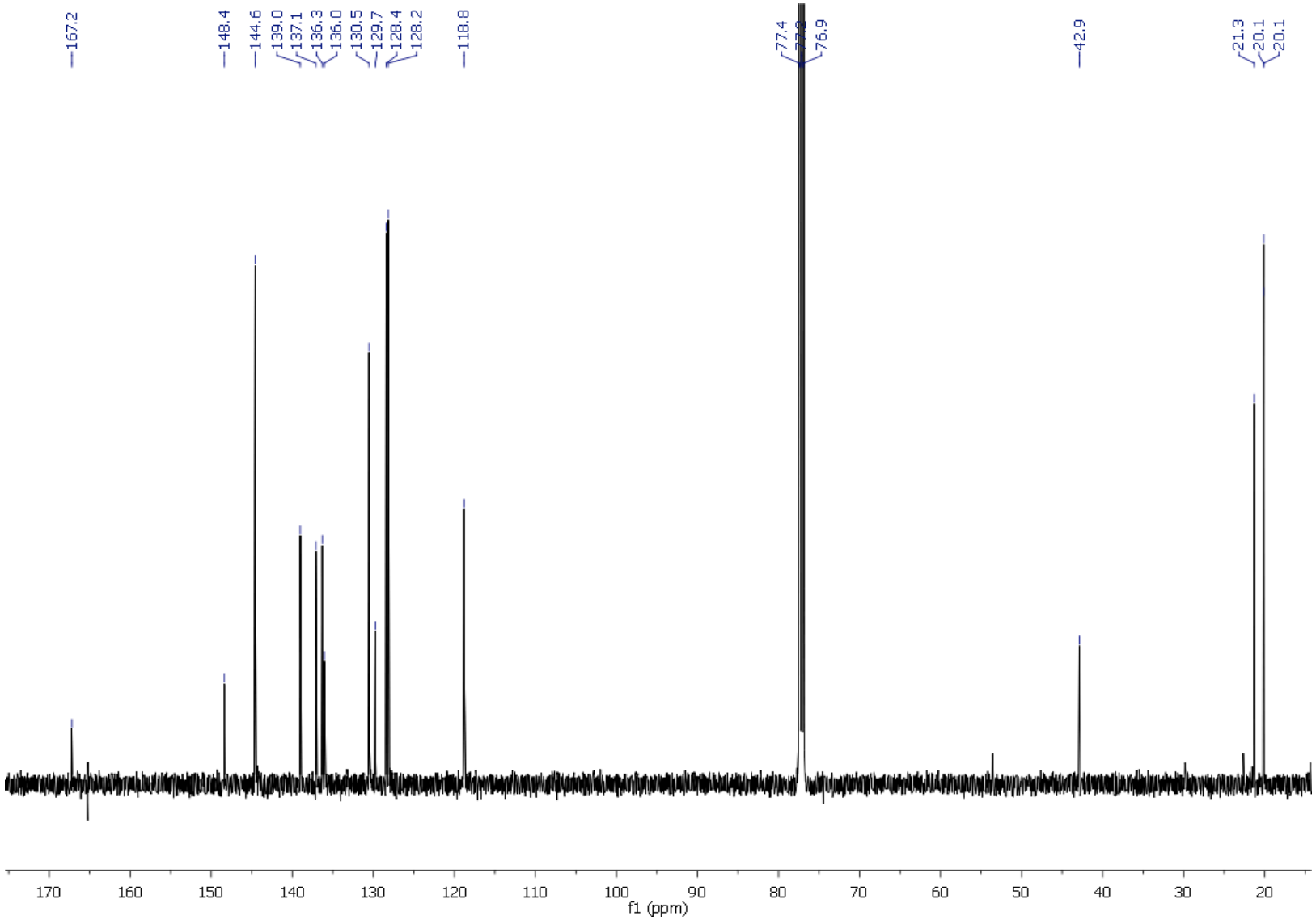

^{13}C NMR (125 MHz, $CDCl_3$) spectrum of compound **2i**

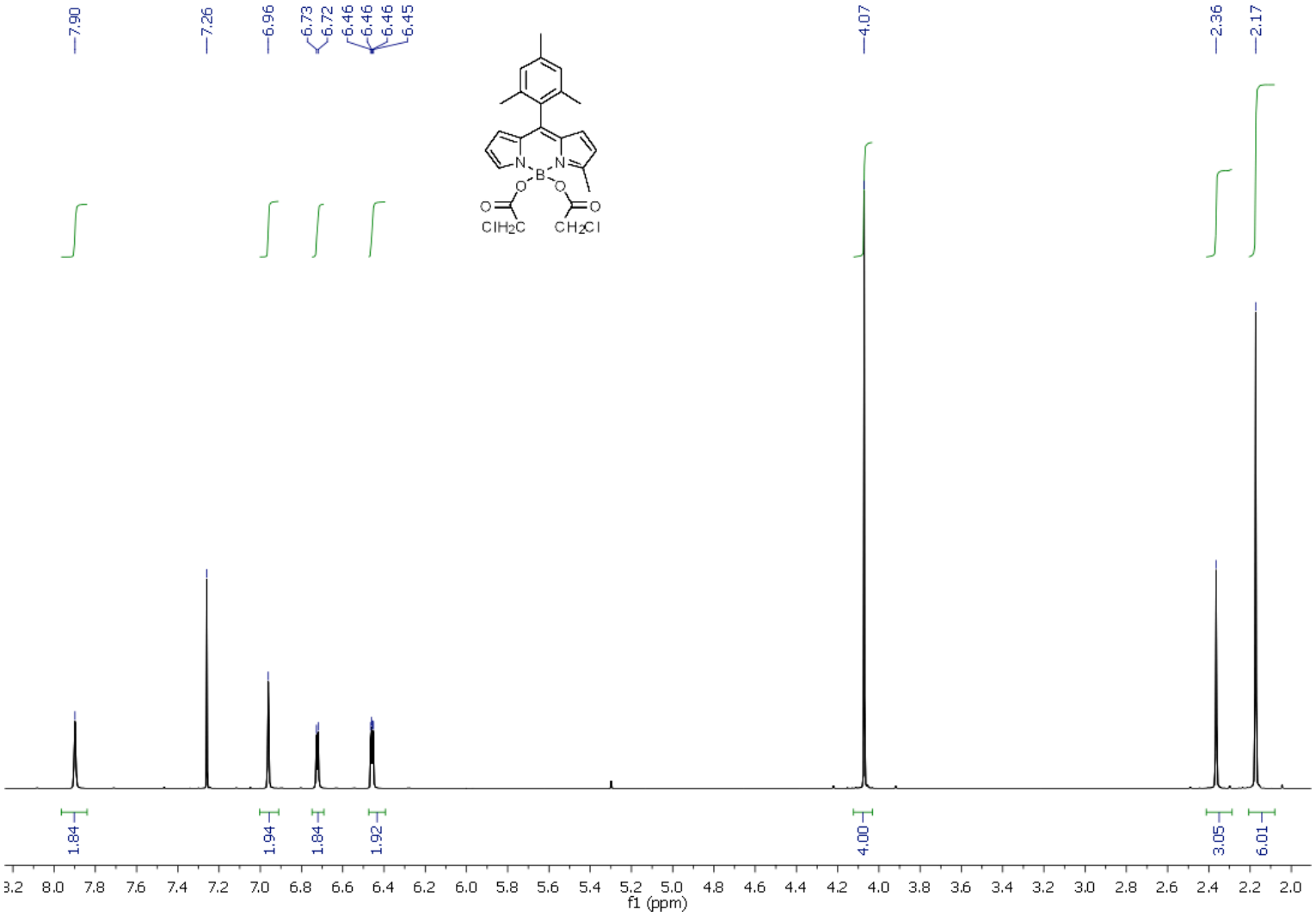

^{1}H-NMR (500 MHz, $CDCl_3$) spectrum of compound **2j**

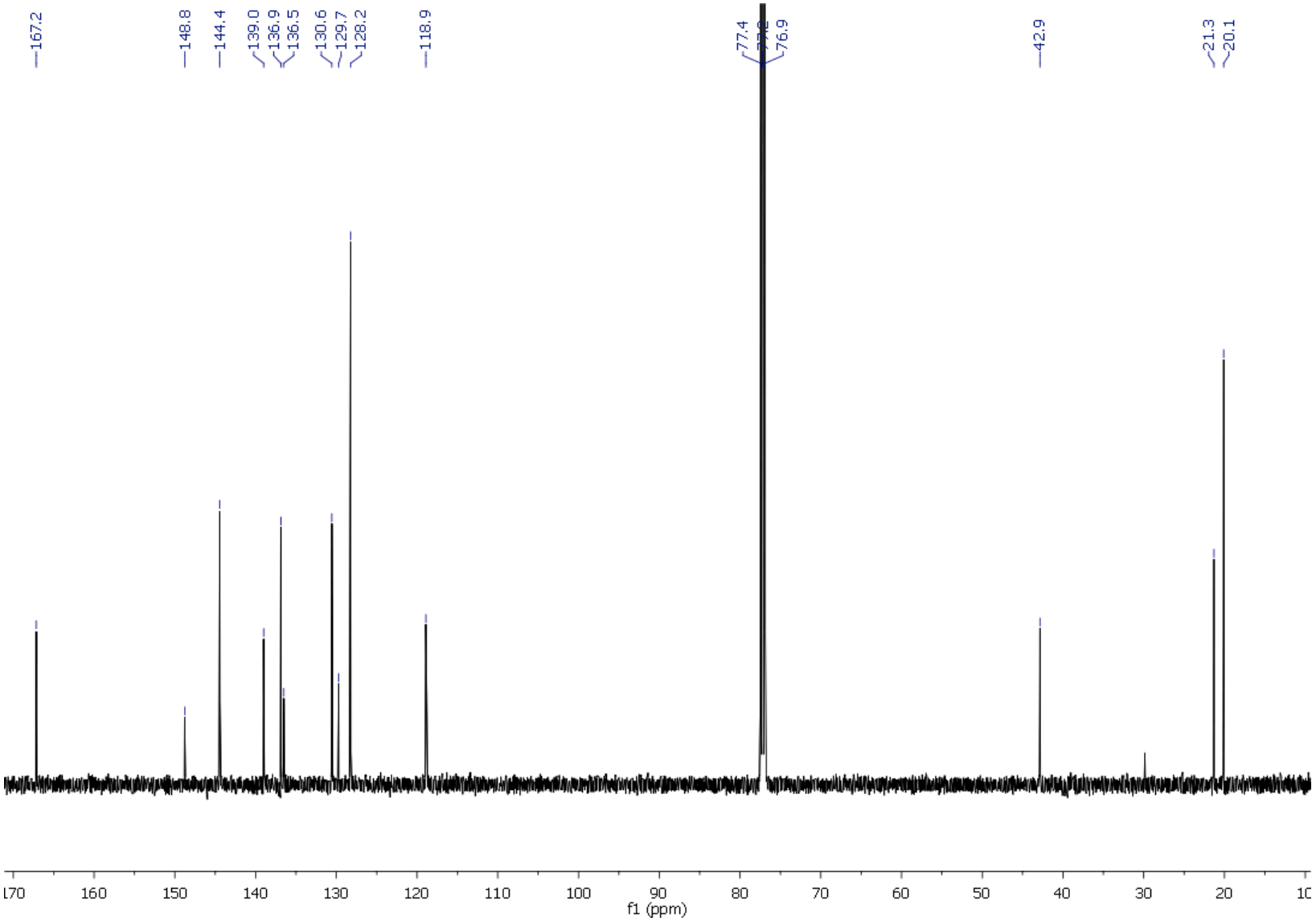

^{13}C NMR (125 MHz, $CDCl_3$) spectrum of compound **2j**

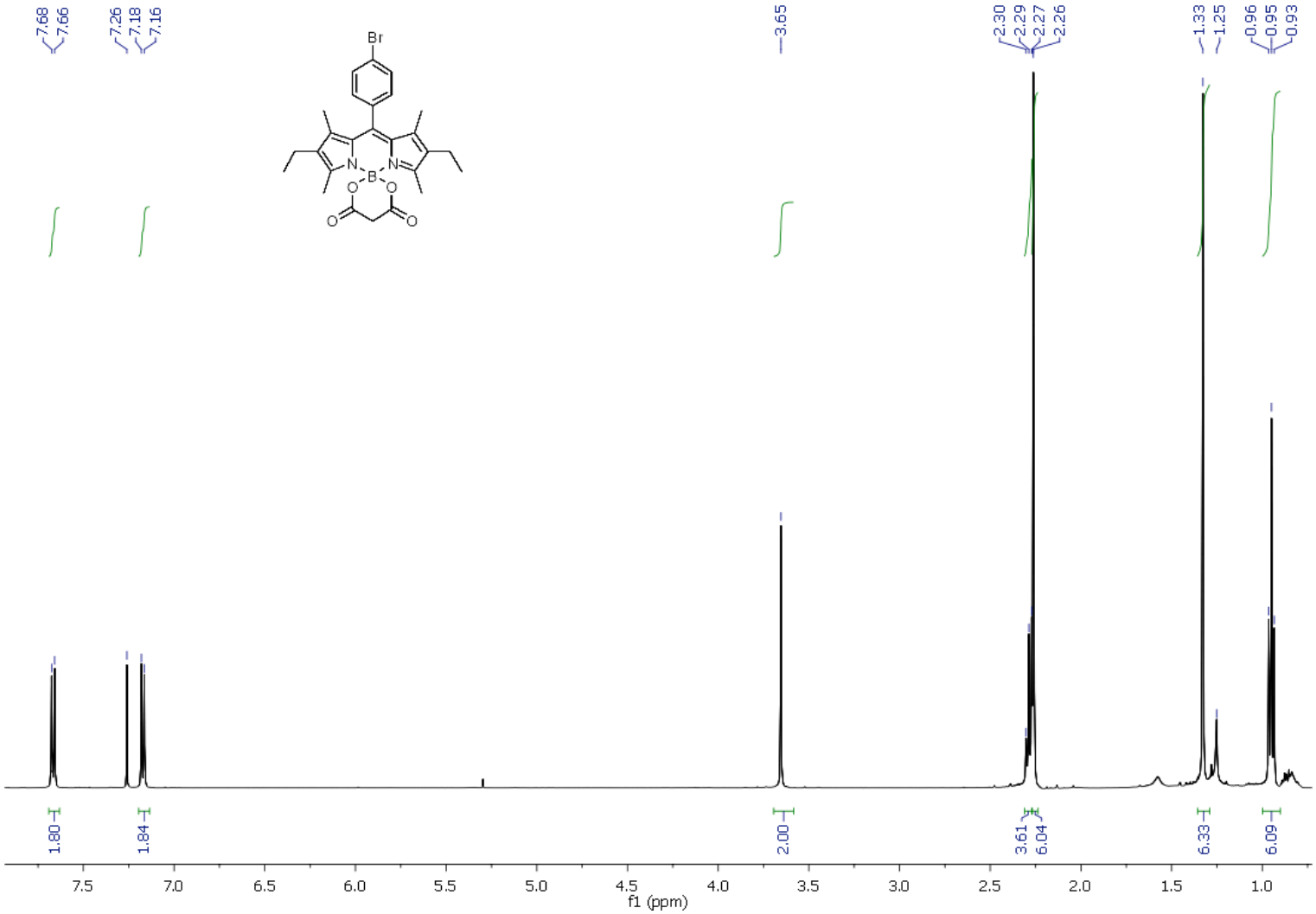

^{1}H NMR (500 MHz, $CDCl_3$) spectrum of compound **3a**

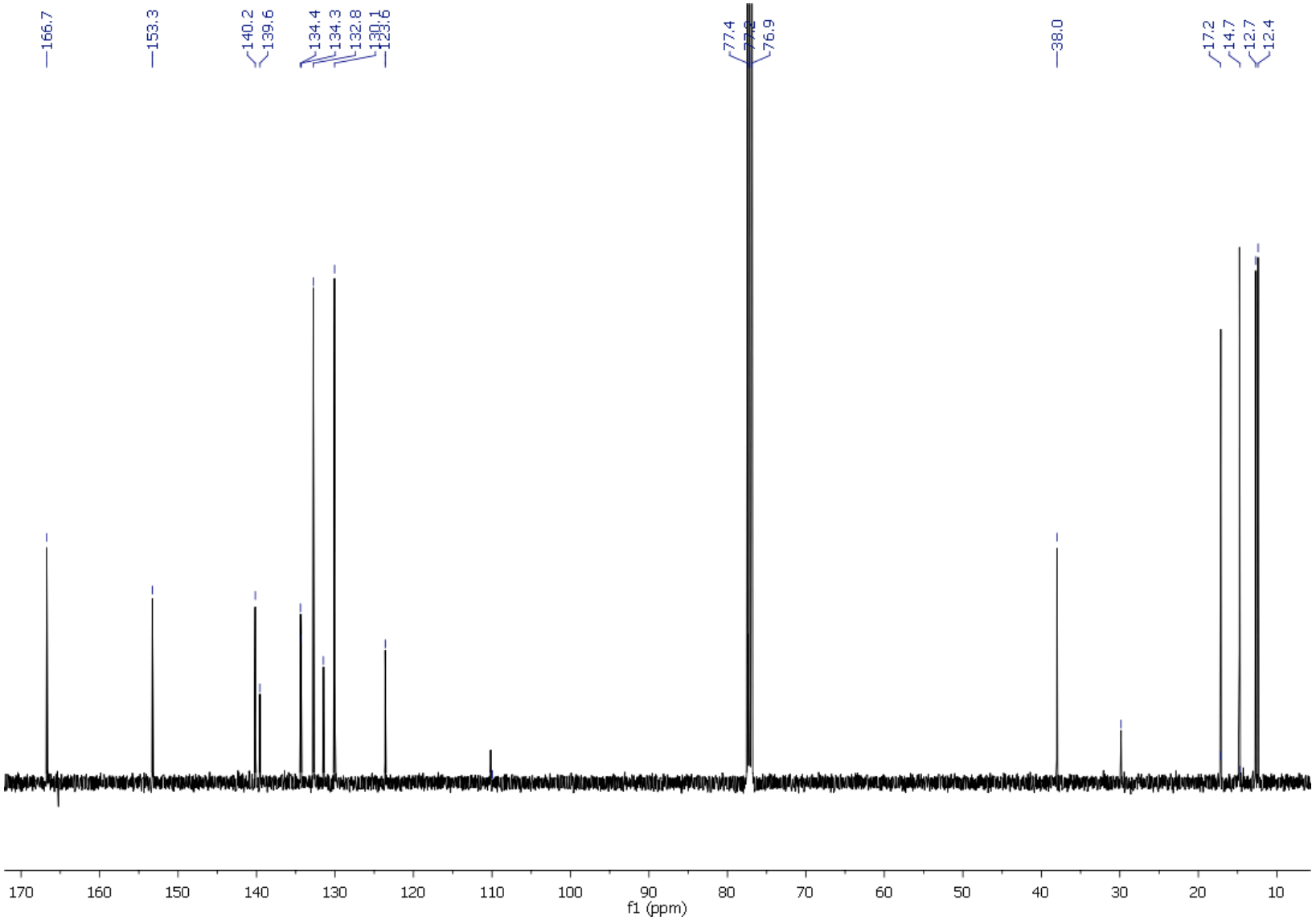

^{13}C NMR (125 MHz, $CDCl_3$) spectrum of compound **3a**

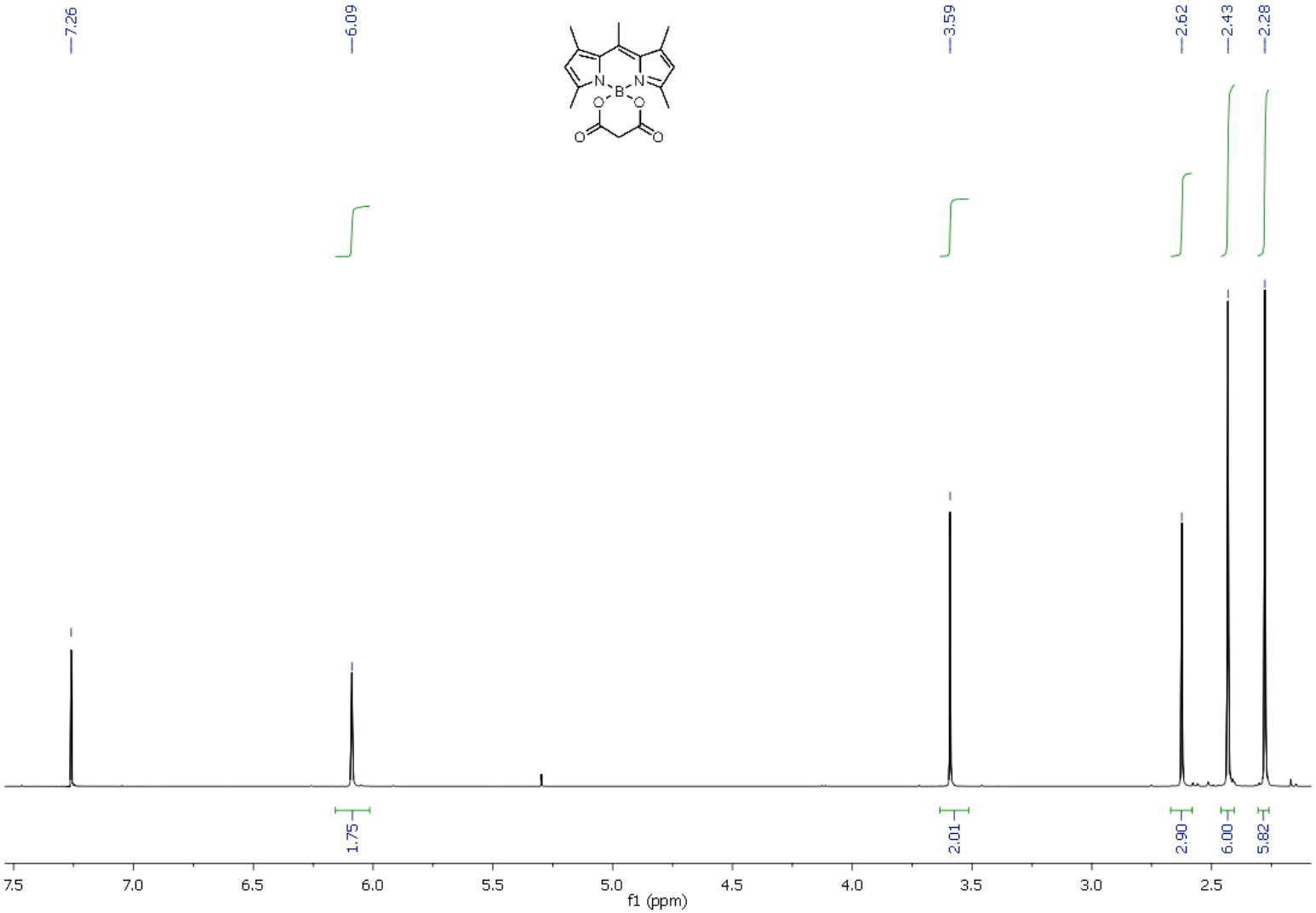

^{1}H NMR (500 MHz, $CDCl_3$) spectrum of compound **4a**

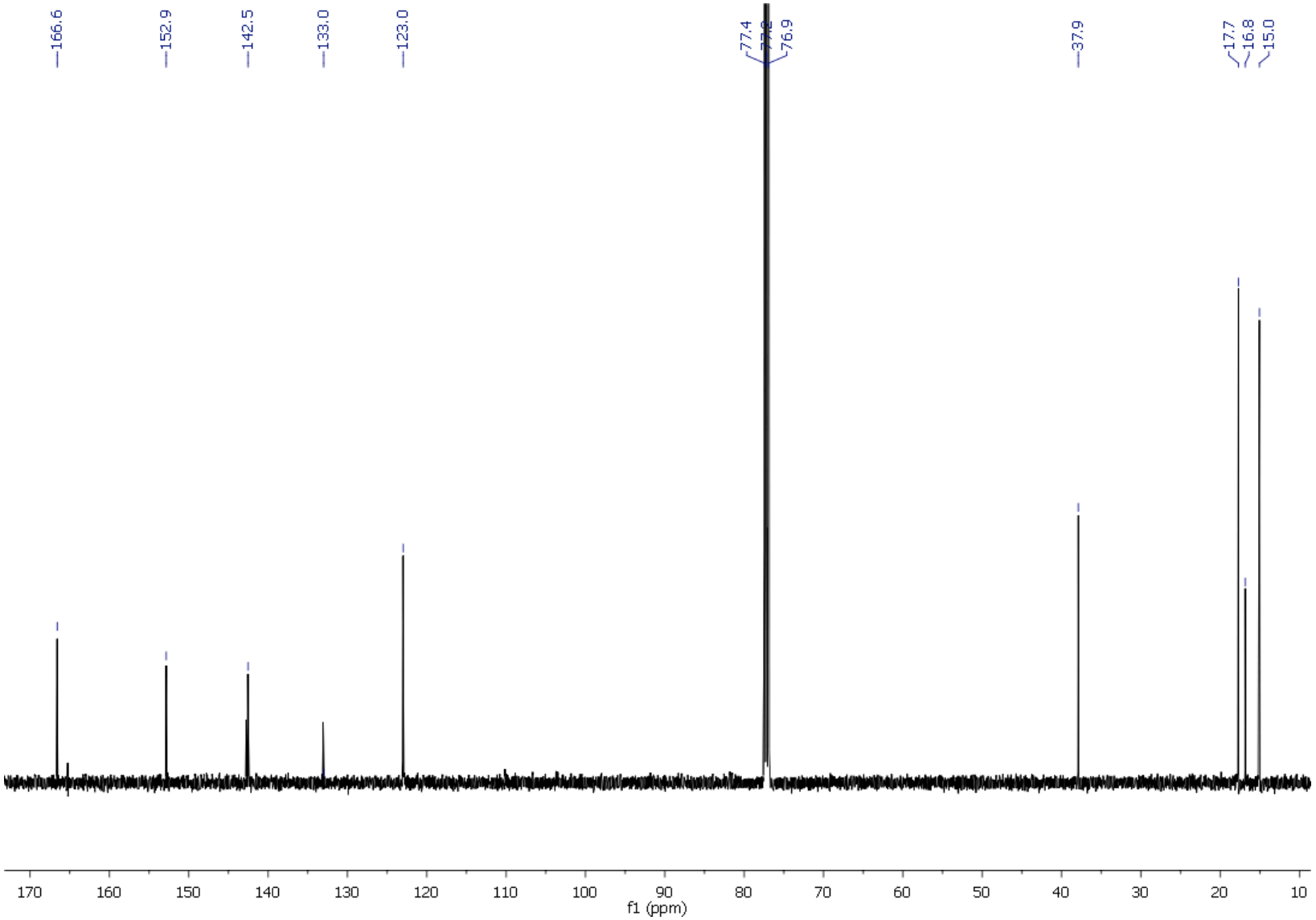

^{13}C NMR (125 MHz, $CDCl_3$) spectrum of compound **4a**

5. References

[1] F. Lopez Arbeloa, J. Banuelos, V. Martinez, T. Arbeloa, I. Lopez Arbeloa, *Int. Rev. Phys. Chem.* **2005**, *24*, 339.

[2] S. L. Mayo, B. D. Olafson and W. A. Goddard, *J. Phys. Chem*. **1990**, *94*, 8897.

[3] M. J. Frisch, G. W. Trucks, H. B. Schlegel, G. E. Scuseria, M. A. Robb, J. R. Cheeseman, G. Scalmani, V. Barone, B. Mennucci, G. A. Petersson, H. Nakatsuji, M. Caricato, X. Li, H. P. Hratchian, A. F. Izmaylov, J. Bloino, G. Zheng, J. L. Sonnenberg, M. Hada, M. Ehara, K. Toyota, R. Fukuda, J. Hasegawa, M. Ishida, T. Nakajima, Y. Honda, O. Kitao, H. Nakai, T. Vreven, J. A. Jr. Montgomery, J. E. Peralta, F. Ogliaro, M. Bearpark, J. J. Heyd, E. Brothers, K. N. Kudin, V. N. Staroverov, R. Kobayashi, J. Normand, K. Raghavachari, A. Rendell, J. C. Burant, S. S. Iyengar, J. Tomasi, M. Cossi, N. Rega, N. J. Millam, M. Klene, J. E. Knox, J. B. Cross, V. Bakken, C. Adamo, J. Jaramillo, R. Gomperts, R. E. Stratmann, O. Yazyev, A. J. Austin, R. Cammi, C. Pomelli, J. W. Ochterski, R. L. Martin, K. Morokuma, V. G. Zakrzewski, G. A. Voth, P. Salvador, J. J. Dannenberg, S. Dapprich, A. D. Daniels, Ö. Farkas, J. B. Foresman, J. V. Ortiz, J. Cioslowski, D. J. Fox, Gaussian 09, Revision B.01, Gaussian, Inc., Wallingford CT, 2009.

[4] C. M. Breneman, K. B. Wiberg, *J. Comput. Chem*. **1990**, *11*, 361.

[5] S. Plimpton, *J. Comput. Phys*. **1995**, *117*, 1.

[6] W. Shinoda, M. Shiga, M. Mikami, *Phys. Rev. B* **2004**, *69*, 134103.

[7] S. J. Plimpton, A. P. Thompson, *MRS Bull*. **2012**, *37*, 513.

[8] L. Martínez, R. Andrade, E. G. Birgin, J. M. Martínez, PACKMOL: A package for building initial configurations for molecular dynamics simulations; Wiley Subscription Services, Inc., A Wiley Company, 2009; Vol. 30, pp. 2157.

[9] M. Brehm, B. Kirchner, *J. Chem. Inf. Model*. **2011**, *51*, 2007.

[10] I. Shoshan, N. N. Danon and U. P. Oppenheim, *J. Appl. Phys*. **1977**, *48*, 4495.

[11] CrysAlisPro, Agilent Technologies,Version 1.171.37.31 (release 14-01-2014 CrysAlis171.NET) (compiled Jan 14 2014,18:38:05).

[12] O.V. Dolomanov, L. J. Bourhis, R. J. Gildea, J. A. K. Howard and H. Puschmann, *J. Appl. Cryst.* **2009**, *42*, 339.

[13] G. M. Sheldrick, *Acta Cryst.* **2008**, *A64*, 112.

[14] C. F. Macrae, I. J. Bruno, J. A. Chisholm, P. R. Edgington, P. McCabe, E. Pidcock, L. Rodriguez-Monge, R. Taylor, J. van de Streek and P. A. Wood, *J. Appl. Cryst.* **2008**, *41*, 466.

[15] A. L. Speck, "PLATON, a multipurpose crystallographic tool." Utrecht University, Utrecht, The Netherlands, 2001, http://www.cryst.chem.uu.nl/platon/. Spek, A. L. *Acta Cryst.* **2009**, *D65*, 148.

[16] L. J. Farrugia, *J. Appl. Cryst.* **1999**, *32*, 837.